ISSN-1560-604X
Thermology international

Thermology International

Volume 18 (2008)
Number 4 (October)

The Glamorgan Protocol

Pain habituation after cold immersion

21st Themological Symposium: Abstracts

Published by the
European Association of Thermology
and the
Austrian Society of Thermology

This journal is indexed in
EMBASE/Excerpta Medica

THERMOLOGY INTERNATIONAL

Volume 18 (2008) **Number 4 (October)**

Published by the
Austrian Society of Thermology and European Association of Thermology

Indexed in
Embase/Excerpta Medica

Organ of the American Academy of Thermology

Organ of the Brazilian Society of Thermology

Organ of the European Association of Thermology

Organ der Deutschen Gesellschaft für Thermologie

Organ of the Polish Society of Thermology

Organ der Österreichischen Gesellschaft für Thermologie

Organ of the UK Thermography Association (Thermology Group)

Contents (INHALTSVERZEICHNIS)

Review (ÜBERSICHT)

Original article (ORIGINALARBEIT)

News in Thermology (THERMOLOGISCHE NACHRICHTEN)

Meetings (VERANSTALTUNGEN)

The Glamorgan Protocol for recording and evaluation of thermal images of the human body

Kurt Ammer

Institute for Physical Medicine and Rehabilitation, Hanuschkrankenhaus, 1140 Wien, Austria
Medical Imaging Research Unit, Faculty of Advanced Technology, University of Glamorgan, Pontypridd, UK

SUMMARY

The historical development of standards for medical thermal imaging in Europe, Northern America and the Far East is reported. Few studies were found in the literature which studied normal temperature values in selected body regions or focused on the symmetry of temperature distribution on the body surface. Reliabilty or reproducibility of temperature readings from infrared images was not investigated until the Nineties of the 20th Century. However, possible measurement errors to to oblique views on an object were identified in the Nineteen-Seventies.

A set of views of body positions and regions of interest in these views was developed for the project of an atlas of normal infrared images of healthy subjects. A number of excperiments was performed to proof both the reproducibility of views for various body positions and the reliability of temperature readings from the defined regions of interest. Some modifications of the views on hands, knees and ankles wer made based on these studies. A high level of reproducibility of temperature readings was obtained for the selected shapes of regions of interest on hands, arms,the upper back, knees,ankles and feet. The Glamorgan Protocol, strictly applied for image recording and evaluation, increases the reproducibilty of findings from thermal images.

KEY WORDS: Standard procedures, thermal imaging, field of views, regions of interest

DAS GLAMORGAN PROTOKOLL FÜR DIE AUFNAHME UND AUSWERTUNG VON WÄRMEBILDERN DES MENSCHLICHEN KÖRPERS

Die Geschichte der Entwicklung von Standards für die medizinische Thermographie in Europa, Nordamerika und Fern-Ost wird berichtet. In der Literatur fanden sich nur wenige Studien die Temperatur-Normwerte ausgewählter Körperregionen untersuchten oder auf die symmetrische Temperaturverteilung an der Körperoberfläche ausgerichtet waren. Die Zuverlässlichkeit oder die Wiederholbarkeit von Temperaturwerten aus Wärmebildern wurdene erst in den neunziger Jahren des 20. Jahrhunderts untersucht. Allerdings wurden mögliche Messfehler auf Grund eines nicht rechtwinkeligen Strahlengangs bereits in den Neunzehn-Siebzigern wahrgenommen.

Für die Enticklung eines Atlas normaler Wärmebilder gesunder Personen wurde eine Reihe Aufnahmepositionen für Körperregionen entwickelt und in diesen Bildausschnitten Messareale definiert. Eine Reihe von Untersuchungen wurden dann durchgeführt., um die Wiederholbarkeit der Bildauschnitte verschiednere Körperpositionen und die Zuverlässlichkeit von Temperaturwerten aus den definierten Messarealen zu beweisen. Diese Studien führten zur Modifikation der Bildausschnitte für Hände, Knie und Sprunggelenke. Die ausgelesenen Temperaturen aus den Messarealen an den Händen, Armen, dem oberen Rücken, Knie, Sprunggelenken und Füßen zeigten ein hohes Maß von Reproduzierbarkeit. Wenn das Glamorgan Protokoll konsequent für die Aufnahme und Auswertung von Wärmebildern befolgt wird, wird die Reproduzierbarkeit der Ergebnisse der Infrarotthermographie vermehrt.

Schlüsselwörter: Standardprozeduren, Thermographie, Bildausschnitt, Messareale

Thermology international 2008: 18: 125- 144

Introduction

Infrared thermal imaging has been used in medicine since the early 1960's. Working groups within the European Thermographic Association (now European Association of Thermology) produced the first publications on standardisation of thermal imaging in 1978 [1] and 1979 [2]. However, ideas for standardisation of thermal imaging appeared including patient preparations, gray scale orientation (white or black may represent high temperatures) can be found in a monograph on Clinical Thermography written by the American radiologist J.D. Wallace and the English physicist CM Cade and published by CRC press in 1975 [3]. Collins and Ring developed methods for quantitation of infrared images as early as 1970 [4] and established in 1974 a quantitative thermal index [5], which was modified in Germany by J-M. Engel in 1978 [6]. Both indices opened the field of quantitative evaluation of medical thermography..

Further recommendations for standardisation appeared in 1983 [7] and 1984, the later related to essential techniques for the use of thermography in clinical drug trials [8]. J-M.Engel published a booklet entitled "Standardised thermographic investigations in rheumatology and guideline for evaluation" in1984 [9]. The author presented his ideas for standardisation of image recording and assessment including some normal values for wrist, knee and ankle joints. Engel´s measurements of knee temperatures were first published in 1978 [5]. Normal temperature values of the lateral elbow, dorsal hands, anterior knee, lateral and medial malleolus and the 1st metatarsal joint were published by Collins in 1976 [10] Acciarri et al. [11} published normal temperature distribution in hands by describing the percentage of hot and cold areas in the carpal and metacarpal regions, over metacarpo-phalangeal joints and fingers. Ammer et al. [12] reported temperature values of small finger joints in healthy subjects and in patients with osteoarhritis, carpal tunnel syndrome or Raynauds´s phenomenon. Francis Ring reviewd the principles, technology, standards, medical applications and results of quantitative thermal imaging in 1990 [13] Clark & Goff updated the EAT-1979- terminology and standards in 1997 [14]. Ring & Ammer summarised the achievements in standardisation for thermal imaging in 1999 [15] and updated this review for the infrared chapter of the Bioengineering Handbook in 2006 [16].

The American Academy of Thermology published technical guidelines in 1986 including some recommendations for thermographic examinations [17]. However, the American authors concentrated on determining the symmetry of temperature distribution rather than the normal temperature values of particular body regions. Uematsu in 1985 [18] and Goodman 1986 [19] published the side to side variations of surface temperatures of the human body. These symmetry data were confirmed by E.F. Ring for the lower leg in 1986 [20]. Two little studies, based on the standard protocol for image recording and evaluation that was developed at the University of Glamorgan, found also highly symmetrical temperature distribution in the upper [21] and lower extremitiers [22]. The clinical importance of temperature asymmetry at the knee was recently reviewed and the paucity of publication related to temperature symmetry was criticised [23]. Based on liquid crytal contact thermography, a high level of symmetric temperature distribution was shown for the cervical spine and the upper extremities [24].

In Japan, medical thermal imaging has been an accepted diagnostic procedure since 1981 [25] Recommendations for the analysis of neuromuscular thermograms were published by Fujimasa et al in 1986 [26]. 5 years later. more detailed proposals for the thermal image based analysis of physiological functions were published in Biomedical Thermology [27], the official journal of the Japanese Society of Thermology. This paper was the result of a workshop on clinical thermography criteria.

The thermography societies in Korea have published a book, which summarizes on 270 pages general standards for imaging recording and interpretation of thermal images in various diseases [28]-

The International Academy of Thermology (IAOCT), a society where most members are chiropractors, has copied and adapted the standards and procedures [29] which were developed in Europe [1,2,14) and Japan [26]. Recently, the American Academy of Thermology published Guidelines for Neuromuscular Thermograpy [30] which are partly based on the previous technical guidelines [17].

Cold challenge

Increasing the thermal contrast by cooling of the skin has a long tradition in thermal imaging. Particularly in breast thermography, a cooling fan [31, 32], somtimes in combination with a cooling liquid [33], or alcohol spraying)34,35) were used for that purpose. Di Carlo used a contact cooling device to enhance the thermal contrast in patients with skin disorders [36]- Cooling with a fan was also applied in thermal imaging of patients with tennis elbow (37).

However, the most common temperature challenge is the immersion of the hands in cold water. Various temperatures were used for the bath water ranging from ice water to 20 degrees C°[38]. Immersion in cold water is common provocation test for vasospastic disease of the fingers i.e. Raymaud´s Phenomenon [39]. Francis Ring described a Thermal Index by computing the differences of the mean temperatures of the dorsum of the hand and of all fingers prior and post cold challenge [40]. A negative figure of 4 or more indicates Raynaud´s Phenomenon. A mild cold challenge was also used to detect inflamed osteoarthritis of finger joints [12] or carpal tunnel syndrome [41].

Immersion of hands or feet in ice water was used in breast thermal imaging following the idea that vessels of a malign tumour do not follow the regulations of the autonomic nerve system and will therefore resist to constrict and increase in that way the thermal contrast of the affected breast. However, an advantage of that test compared to the standard image recording was never proven [33].

Reliability of thermal imaging

Early attempts to investigate the reliabilty of thermal imaging were focused on equipment and errors related to to the principles of physics applied in thermal imaging.. Emissivity and loss of infrared radiation beyond an angle of 45 to 60 degrees were indentified as sources of error in the Nineteen-Seventies (42-45). Resolution of thermal imagers was adressed in 1972 when the dependence of temperature resolution from spatial resolution was clearly demonstrated [46]. Francis Ring used an heated resolution chart to investigate the temperature and spatial resolution of infrared imagers in 1982 [47] and repeated these experiments in 1999 with modern equipment of that time [48]. Two papers from Austria investigated the relationship between spatial resolution and distance between an human object and and the recording thermal imager. [49,50]. Michael Anbar adressed in 1991 [51] again the physics of infrared imaging in response to a paper by Ash et al. [52] where thermal imaging was found to be neither accrurate nor precise. Ammer described potential pitfalls in recording and evaluation of medical thermal images related to imaging equipment, patient preparation and image interpretation [53]. Recently, the Medical Imaging Research Unit at the University of Glamorgan described a series of simple tests for checking infrared cameras to improve the reliabilty of thermal imaging [54].

The reproducibilty of a qualitative evaluation of thermal images from hands suspected of complex regional pains syndrome (CRPS) type 1 was recently published.[55]. The authors obtained a diagnostic sensitivity of 71% and a specificity of 85% for thismethod , but only moderate repeatability (0.53) and reliability was 0.50. Temperature measurements from total body images found high reproducibility in the body core regions and poor repeatabilty in the periphery of the body [56]. A veterinary paper reported that the thermal pattern of the horse back did not change during acclimatisation time and stays stable for 7 days.[57]. However, the absolute temperature values varied during acclimatisation and were affected by hair coat and environmental factors

Few papers were related to variation of temperature measurements due to shape and size of measurement areas. Melnizky et al investigated the intra-and intrarater repeatabilty of temperature measurements from thermograms of patients suspected to suffer from thoracic outlet syndrome and reported narrow confidence intervals of repeated measurements [58]. H.Mayr compared in knees the mean temperatures of small rectangular measurement areas with the mean temperature of a line and found good correlation between these two methods of quantitation [59]. A significant different temperature readings occurs when the number of pixels within the region of interest varies by 100 or more percent [60].. Although the close correlation of .temperature readings from small or large measurement areas from the same thermal image was confirmed in the evaluation of patients with Thoracic Outlet Syndrome[61] or Raynaud´s phenomenon [62], further measurements derived from these readings will affect the diagnostic power of infrared thermal imaging [63].

Other papers related to the repetability of field of views or reproducibility of temperature readings from defined regions of interest were conducted to control the methodology used in the Glamorgan Protocol for recording and evaluation of thermal images of the human body.

The Glamorgan Protocol

In 2001, the project "Atlas of normal skin temperature distribution was started to close the gap in knowledge of distribution of skin temperature in healthy subjects.The first step was to define 24 body views (Appendix I) The principle was to depict as much as possible of the anatomical region of interest. To achieve this, anatomical landmarks were aligned in each view to the edge of the image. In that way , the same view of the body region was achieved irrespective of the body proportion of the subject imaged. The aim of these definitions was to reproduce the views of body positions as close as possible and to increase in that way the reproducability of thermal imaging.

Consequently , the variation in body views was investigated using thermal images recorded from subjects for the the atlas of normal skin temperature distribution. As the thermal images were taken by four different camera operators, . it was possible to investigate the intra- and inter- investigator variation of body views. The distance between the ana tomical landmarks and the closest edge of the thermal image was measured by the numbers of pixels using the crosssection tool of the Ctherm Software Package. [64, 65].

The smallest variation was found for the body views "Face" and "Upper Back" and the biggest variation was found in hands, knees and ankles leading to revision of the recording rules of these images (table 1).

The repeatabilty of the the view of the revised view "dorsal hands" was investigated in the practical session of an instructional course in medical thermal imaging [66]. 14 participants twice recorded the dorsal hands of a volunteer with an infrared thermal imager. The mean size of the hands, measured in pixel, was about 40000 and varied in repeated image capture in one group by approximately 2300 pixel, and by 600 in the other group. However, there were individual deviations from the mean size of the hands in the range of 5000 to 7600 pixel. During another Training Course for Medical Thermal Imaging, two separate thermal images using the standard view "Face"were recorded from one subject by 8 participants [67]. The size of the imaged field of view varied from 0.2 to 3,7% of the number of pixels within the object imaged. Deliberate variations in the views "face" and "upper back" view lead to significant differences in temperature readings from these images. [68] temperature readings

The Glamorgan protocol defined also 90 regions of interest (Appendix II).The repeatabilty of temperature readings from selected measurement areas was evaluated in relationship to the shape of the region of interest.

Comparison of a rectangular, a circular and an hour-glas shaped region of interest in the viewa "Both Knees Anterior" obtained the highest repeatabilty of temperature readings in the hour glass shape which can more easely aligned to anatomical landmarks than the two other competing shapes [64]. Temperature readings from the circular regions on the soulder in the view "Upper Back" were better reproduced than the temperature values from an polygon shaped measurement area. [68]. In the view "Anterior Arm" the highest repeatability of temperature measurements was obtained for the region of interest "Anterior Forearm" with reliabilty coefficient alpha of 0, 927 [65]. Reliability coefficients for the views "Both Ankles Anterior", "Dorsal feet" and "Plantar feet" ranged between 0.7 (right ankle) and 0.95 (left ankle).

Table1
Variation of positions of all the investigated views [16]

View	Upper edge (pixel) mean ± SD (95% CI)	Lower edge (pixel) mean ± SD (95% CI)	Left side edge (pixel) mean ± SD (95% CI)
Face	0.5 ± 5.3 (-2.2.to 1.9)	4.0 ± 10.9 (-.03 to 8.2)	
Dorsal Neck	-8.4 ± 36.4 (-18.3 to 1.6)	122.6 ± 146.6 (82.6 to 162.6)	
Upper Back	4.5 ± 9.9 (0.8 to 8.2)	28.1 ± 22.0 (19.9 to 36.4)	
Anterior Left Arm	22.4± 33.0 (8.7 to 36.0)	15.8 ± 15.4 (9.5 to 22.2)	12.5 ± 16.0 (5.9 to 19.1)
Dorsal Hands	41.8 ± 17.8 (35.5 to 48.2)	33.2 ± 22.3 (25.3 to 41.5)	
Both Knees Anterior	80.7 ± 47.3 (60.7 to 100.7)	84.3 ± 37.0 (68.6 to 99.9)	
Lateral Right Leg	16.7 ± 21.0 (5.9 to 27.5)	17.2 ± 15.8 (9.0 to 25.3)	
Lower Back	17.1 ± 4.2 (8.6 to 25.6)	16.3 ± 4.6 (16.3 ro 34.9)	
Both Ankles Anterior	158.8 ± 12.2 (133.6 to 184.1)	54.9 ± 9.1 (36.1 to 37.8)	
Plantar Feet	31.0 ± 24.1 (23.2 to 38.7)	25.7 ± 23.1 (18.3 to 33.1)	

A remarkable small standard deviation of mean temperatures of small joints of fingers was obtained in repeated measurements performed by a group of newly trained thermographers [66]. However, individual errors of measurement up to 2.3°C were seen across the group as a whole. The use of a template for the placement of regions of interest increases the reproducibility of temperature readings. However, such a template cannot overcome measurement errors caused by variations in body positioning. In an otherv training group, temperature readings from region of interest "Right Forehead" were also reproduced on a high level, but in two readers the temperature values were significantly different in repeated evaluation [67].

Discussion

The Glamorgan Protocol, developed to generate reference images for an "Atlas of Infrared Images of Healthy Subjects " has proven that both the definition of the field of views for body positions and the regions interest provide high reproducibilty of recorded images and temperature readings. The protocol was applied already in studies which are not related to the Atlas Project [69,70,71]..

The proposed procedures of image recording and evaluation do not claim to be comprehensive, but when strictly applied, an important source of error and unreliabilty of thermal imaging can be avoided. Any other body position for image recording is possible, but the degree of reproducibility of alternative views must be tested in a similar manner as it was done for the Glamorgan Protocol. This protocol allows only to control for variation in camera views on body position and placement of regions of interest. Other factors due to patients preparation and temperature control of the examination room may also contribute to poor reliability of thermal images.

Some problems may arise from the infrared equipment, which must be regularly checked for malfunction. The battery of tests [54], developed by the members of the Medical Imaging Research Unit at the University of Glamorgan, provied means for an easy and unexpensive quality control of infrared imagers.

Reliability of measurements is one of the main features of outcome measures. There is now sufficient evidence that thermal imaging is a reliable outcome measure [72] which may be used in a variety of medical applications.

References

1.Aarts NJM et al. Thermographic Terminology. Acta Thermographica. 1978 Supplement 2

2.Engel JM, Cosh JA, Ring EFJ, Page Thomas DP, Van Waes P, Shoenfeld D. Thermography in Locomotor Diseases - Recommended Procedure. Eur. J Rheum. Inflamm 1979; 2: 299-306.

3.WallaceJD, Cade CM. Clinical Thermography. CRC Press, Cleveland, 1975 .

4.Collins AJ , Ring EFJ , Cosh JA, BaconPA. Quantitation of thermography in arthritis using multi-isothermal analysis. Ann. Rheum. Dis. 1974; 33, 113-115

5.Engel, J.-M. Quantitative Thermographie des Kniegelenks. Z.Rheumatol. 1978, 37, 242-253.

6. Ring EFJ, Collins AJ. Quantitative Thermography. Rheumatology and Physical Medicine 1970, 10(7), 337- 341

7.Ring, E.F.J. Standardisation of Thermal Imaging in Medicine: Physical and Environmental factors, in Thermal Assessment of Breast Health. Gautherie, M., Albert, E., and Keith, L., Eds., MTP Press Ltd, Lancaster/Boston/The Hague, 1983. 29

8 Ring EFJ., Engel JM, Page–Thomas DP. Thermologic methods in Clinical Pharmacology - Skin Temperature Measurement in Drug Trials. Int. J. Clin. Pharm. Ther Tox., 1984;22, 20,

9.Engel J-M, Saier, U. Thermographische Standarduntersuchungen in der Rheumatologie und Richtlinien zu deren Befundung. Luitpold, München, 1984

10.CollinsAJ. Anti-inflammatory drug assessment by the thermo- graphic index. Acta thermographica, 1, 73, 1976

11. Acciarri L, Carnevale F, Della Selva A. Thermography in the hand angiopathy from vibrating tools. Acta thermographica 1976; 1, 18-28.

12.Ammer K, Engelbert B, Kern E. The Determination of Normal Temperature Values of Finger Joints Thermology international 2002, 12: 23-33

13.Ring EFJ: Quantitative thermal imaging. Clin Phys Physiol Meas 1990, 11, Suppl A, 87-95

14.Clark RP, de Calcina-Goff M. Guidelines for Standardisation in Medical Thermography Draft International Standard Proposals. Thermol. Osterr.; 1997; 7, 2, 47-58

15,Ring EFJ, Ammer K. The technique of thermal imaging in medicine. Thermol. Int., 2000, 10, 7-14.

16.Ammer K, Ring F. Standard Procedures for Infrared Imaging in Medicine. In: Bronzino J (ed), Biomedical Engineering Handbook (3rd. Edition) Infrared Imaging Section.. N.A Diakides (ed). CRC Press,2006, 36.1-36-14

17- A Committee on Quality Control and Qualifications of the American Academy of Thermology, "Technical Guidelines , Edition 2", Thermology, 1986, 2, 108-112

18.Uematsu S. Symmetry of Skin Temperatures Comparing One Side of the Body to the Other. Thermology, 1985, 1. 4-9

19.Goodman PH. et al. Normal Temperature Asymmetry of the Back and Extremities by Computer-Assisted Infrared Imaging. Thermology, 1, 195, 1986

20.Bliss , Bulstrode SJ, Evison G, Naddison P. Ring FJ. Investigation of nerve root irritation by infrared thermography, in Back Pain- methods for clinical investigation and assessment, Hukins, DWL, Mulholland RC., Eds., University Press, Manchester, 1986, 63.

21. Vardasca R, Ring EJF; Plassman P, .Jones CD. Thermal symmetry on extremities of normal subjects. In: Plasmann P, Wiltshire R, Al-Begain K. Proceedings of the 1st Student Workshop, Thursday 1st March 2007-Glamorgan Business Center, University of Glamorgan 2007, p.14-18

22.Vardasca R, Ring EJF; Plassman P, .Jones CD. Thermal symmetry and temperature values of healthy volunteers on elbow, neck, shoulder ans wrist. Thermology international 2008, 18; 60

23.Selfe J, Whitaker J, Hardaker N. A narrative literature review identifying the minimum clinically important difference for skin temperature asymmetry at the knee. Thermology international 2008, 18: 41-44

24. Feldman F, Nickoloff EL. Normal Thermographic Standards for the Cervical Spine and Upper Extremities. Skeletal Radiol 1984; 12:235-249

25.Atsumi K High Technology Applications of Medical Thermography in Japan. Thermology, 1985, 1:79-80

26.Fujimasa I. et al. A New Computer Image Processing System for the Analysis of Neuromuscular Thermograms: A Feasibility Study. Thermology, 1986; 1, 221,

27Fujimasa, I.. A proposal for thermographic imaging diagnostic procedures for temperature related physiologic function analysis. Biomed. Thermol., 1991; 11, 269,

28. Lee D-I (ed): Practical Manual of Clinical Thermology. ISBN 89-954013-

29.28. Thermography Guidelines. Standards and protocols in clinical thermographic imaging. International Academy of Clinical Thermology. .2002

30. Practice Guidelines Committee of the American Academy of Thermology. Guidelines For Neuromusculoskeletal Thermography .Thermology international 2006: 5-9

31.Amalu WC, Hobbins WB, Head JF, Elliot RL. Infrared Imaging of the Breast — An Overview. In: Bronzino J (ed), Biomedical Engineering Handbook (3rd. Edition) Infrared Imaging Section.. N.A Diakides (ed). CRC Press,2006, 25.1-25.19

32.Ohashi Y, Uchida I. Applying Dynamic Thermography in the Diagnosis of Breast Cancer.Techniques for Improving Sensitivity of Breast Thermography. IEEE Eng Med Biol Magazine 2000, 19(3):42-51

33.Amalric R, Giraud D, Altschuler JM, Spitalier JM: Value and interest of dynamic telethermography in detection of breast cancer. Acta Thermographica 1976, 1: 89-96..

34.Usuki H., Teramoto S., Komatsubara S, Hirai SI, Misumi T, Murakami M, Onoda Y, Kawashima K., Kino K, Yamashita KI, Matsubara J. of subtraction thermography in the diagnosis of breast disease. Biomed. Thermology, 1991, 11(4), 286–291.

35.Ng EY-K, Sudharsan NM. Effect of blood flow, tumour and cold stress in a female breast: a novel time-accurate computer Simulation. Int J Engineer Med 2001;215(H4):393–404.

36. DiCarlo A. Thermography in patients with systemic sclerosis Thermol Österr 1994, 4(1) 18-24

37. Meknas K, Odden-Miland A, Mercer JB, Castillejo M, Johansen O. Radiofrequency microtenotomy: a promising method for treatment of recalcitrant lateral epicondylitis. Am J Sports Med. 2008; 36(10):1960-1965.

38-Ring, E.F.J. Cold stress test for the hands, in The Thermal Image in Medicine and Biology, Ammer, K., and Ring, E.F.J., Eds, Uhlen-Verlag, Wien, 1995, 237

39. Ring EFJ and Collaborators. Raynaud's Phenomenon: assessment by Thermography Thermology 1988;. 3, 69-73

40.Ring, E.F.J. A thermographic index for the assessment of ischemia. Acta thermographica, 1980, 5, 35,

41. Ammer K. Thermographische Diagnose von peripheren Nervenkompressionssyndromen Thermomed 1991; 7,15-21;

42.Watmouth DJ, Fowler PW, Oliver R. The thermal scanning of a curved isothermal surface. Phys Med Biol 1970, 15, 1-8

43. Salter DC, The Effect of Obliquity in Clinical Thermograms. Phys. Med. Biol., 1976, 21(6); 980-998

44. Clark JA. Effects of surface emissivity and viewing angle on errors in thermography. Acta Thermographica 1976, 1:138-141

45. Martin CJ, Watmough DJ. Thermal scanning of curved surfaces. Acta Thermographica 1977, 2: 18-22

46.Macey D, Oliver J. Image Resolution in infrared thermography Phys Med Biol 1972, 17: 563-571

47.RingEFJ. Quality Control in lnfra red Thermography. In: Ring EFJ.; Phillips B., editors. Recent Advances in Medical Thermology NewYork: PlenumPress, 1984. p.185 -94

48,Ring EFJ, Dicks JM. Spatial resolution of New Thermal Imaging Systems, Thermol. Int., 1999; 9, 7-14.

49.Schartelmüller T, .Ammer K. Räumliche Auflösung von Infrarotkameras Thermologie Österreich 1995, 5: 28-31.

50. Maurer A, .Mayr H. Der Meßabstand als Einflußparameter auf die Reproduzierbarkeit bei IR-Thermographiemessungen. European Journal of Thermology 1998; 8 : 101-103

51.Anbar, M. Potential Artefacts in Infrared Thermographic Measurements. Thermology 1991,.3, 273-274.

52..Ash CJ, Gotti E,Haik CH. Thermography of the curved living skin surface. Missouri Med 1987, 84: 702-708

53. Ammer K. Mißbrauch der thermograpischen Untersuchung ThermoMed 1997;13:, 58-65,

54. Plassmann P, Ring EFJ., . Jones CD. Quality Assurance of Thermal Imaging Systems in Medicine. Thermology international 2006, 16: 10-15

55.Niehof SP, Huygen FJPM., Stronks DL, Klein J , Zijlstra FJ. Reliability of observer assessment of thermographic images in Complex Regional Pain Syndrome type. Acta Orthop. Belg., 2007, 73, 31-37

56. Zaproudina N, Varmavuo V, Airaksinen O, Närhi M. Reproducibility of infrared thermography measurements in healthy individuals. Physiol. Meas. 2008, 29(4) 515-524

57.Tunley BV, Henson FM. Reliability and repeatability of thermographic examination and the normal thermographic image of the thoracolumbar region in the horse. Equine Vet J. 2004; 36(4):306-12

58.Melnizky P, Schartelmüller T., Ammer K. Prüfung der intra- und interindividuellen Verlässlichkeit der Auswertung von Infrarot-Thermogrammen. Eur. J. Thermol., 7, 224-227, 1997

59.Mayr H.Korrelation durchschnittlicher und maximaler Temperatur am Kniegelenk bei Auswertung unterschiedlicher Messareale. Thermol. Österr. 1995; 5, 89-91.

60. Ammer K Temperature readings from thermal images are less dependent on the number of pixels of the measurement area than on variation of room temperature. Thermol int 2005, 15(4): 131-133

61.Ammer K Alternative Evaluation of Thermal Images Captured From Patients Suspected To Suffer From Thoracic Outlet Syndrome. In: Benkö I, Kovacsics I, Lovak I , eds.15th International Conference on Thermal Engineering and Thermo- grammetry (THERMO), Abstracts, Merestechnikai, Automatizalas es informatikaj Tudomanyos Egyrsulet (MATE) Hotechnikai es Termogrammetriai (HT es TGM) Szakosztalya, Budapest, 2007

62. Ammer K Three methods of evaluation of thermal images from patients with suspected Raynaud's phenomenon. Thermology international, 2007; 17: 157

63.Ammer K The sensitivity of infrared imaging for diagnosing Raynaud's phenomenon or Thoracic Outlet Syndrome is dependent on the method of temperature extraction from thermal images. Thermology Int. 2008 18 (3): 81-88

64Ammer K, Ring EFJ, Plassmann P, Jones BF. Rationale for standardised capture and analysis of infrared thermal images. In.Hutten H, Krösel P, eds. Proceedings Part II, EMBEC´02 2. European Medical & Biological Engineering Conference. IFMBE, Graz, 2002, pp.1608-1609

65Ammer K. Need for Standardisation of Measurements, in Thermal Imaging, in Thermography and Lasers in Medicine, Wiecek, B., Ed, Akademickie Centrum Graficzno-Marketigowe Lodart S.A, Lodz, 2003, 13.

66Ammer K, Ring EF Repeatability of the standard view both dorsal hands. Results from a training course on medical infrared imaging. Thermology International. 2004; 14(2):99-102

67Ammer K. Repeatability of temperature measurements at the forehead in thermal images from the standard view "face" Thermol int 2006, 16(4): 138-142

68Ammer K, Ring EF. Influence of the field of view on temperature readings from thermal images. Thermol int 2005, 15(3): 99-103

69. Cholewka A, Drzazga Z, Sieron A Monitoring of whole body cryotherapy effects by thermal imaging: preliminary report. Physica Medica, 2006, 22; 57-62

70.Nica A, Meila A, Dima C. Monitoring Treatment In Patients After Stroke By Thermal Imaging: Study Design. Thermol int 2008, 18(4): 148

71. Steinlein S.Erfahrungen mit IR Imaging in einer orthopädischen Klinik Vortrag beim DGTR / IMVT- Workshop in Wiener Neustadt Medizinische Thermographie und Infrarot Imaging - Brust und Bewegungsapparat am 16.10.2008

72. Ammer K. Influence of Imaging and Object Conditions onTemperature Readings from Medical Infrared Images. Polish Journal of Environmental Studies 2006, 15 (4A) 117-119

Address for Correspondence

Prof Kurt Ammer MD, PhD

Institute for Physical Medicine and Rehabilitation,
Hanuschkrankenhaus, Heinrich Colinstr 30
A-1140 Vienna, Austria

Email: KAmmer1950@aol.com

(Manuscript received 10.7.2008, accepted 10.10.2008)

24 body views

1. Total body (anterior view); Code: TBA

upper edge of the image: the most cranial point of the head
lower edge of the image*:* soles of the feet
other conditions arms and legs slightly abducted, palms point forwards, head is a vertical position, neither rotated nor tilted to the side

THERMAL IMAGE

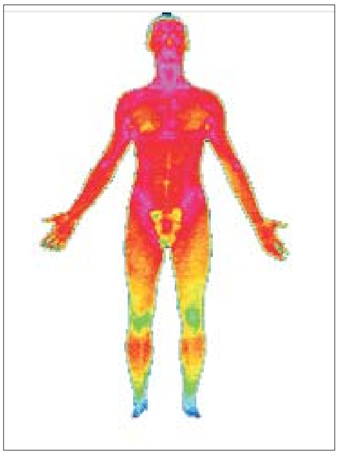

2. Total body (dorsal view); Code: TBD

upper edge of the image: the most cranial point of the head
lower edge of the image*:* soles of the feet
other conditions arms and legs slightly abducted, palms point forwards, head is a vertical position, neither rotated nor tilted to the side

THERMAL IMAGE

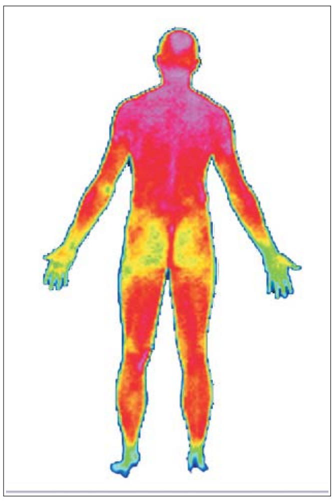

3. Total body (lateral view); Code: TBL (left) or TBR (right)

upper edge of the image: the most cranial point of the head
lower edge of the image*:* soles of the feet
other conditions arms scissored, left hand side of the points towards the camera, head is a vertical position, neither rotated nor tilted to the side

THERMAL IMAGE

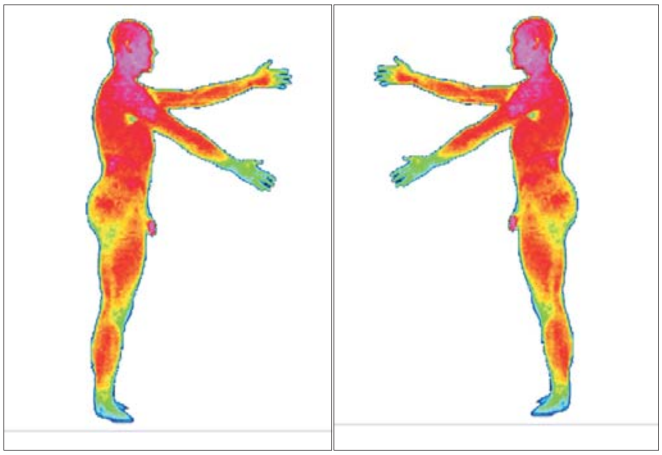

BODY REGIONS

4. Face (anterior view); Code: FA

upper edge of the image: the most cranial point of the head
lower edge of the image*:* below the chin at the level of hyoid bone
other conditions head is a vertical position, neither rotated nor tilted to the side

THERMAL IMAGE

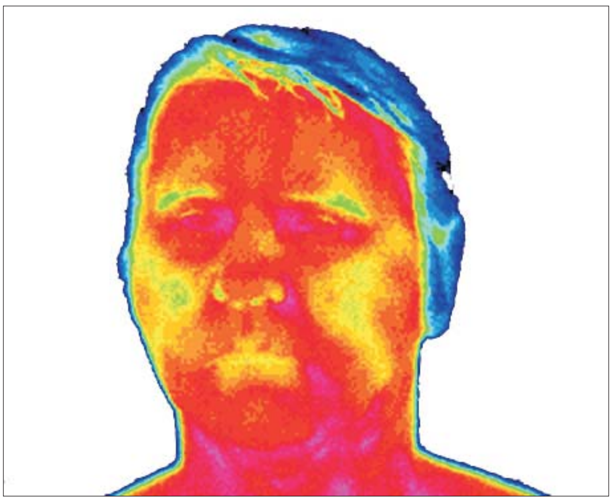

5. Neck (dorsal view); Code: ND

upper edge of the image	line between the cranial ends of the ear
/ower edge of the image:	on the level of the processus spinosus of D1
other conditions	head is a vertical position, neither rotated nor tilted to the side

THERMAL IMAGE

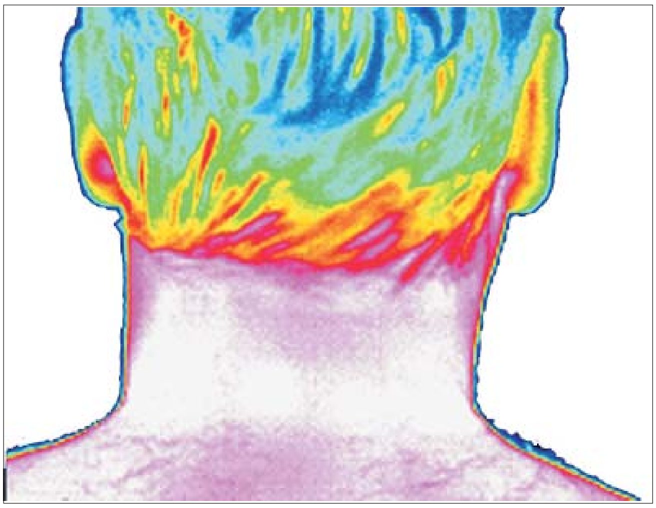

6. Chest (anterior view); Code: CA

upper edge of the image	below the chin at the level of hyoid bone
lower edge of the image:	below the rib cage (approximately the tip of the elbow)
other condition	arms slightly abducted, the outline of both shoulders and upper arms are within the image

THERMAL IMAGE

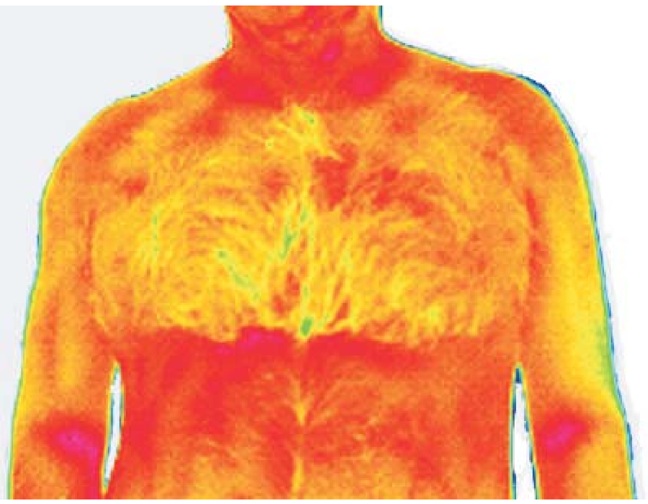

7. Upper Back; Code: UB

upper edge of the image	level of the processus spinosus of C6
lower edge of the image:	below the rib cage (approximately the tip of the elbow
other condition	arms slightly abducted, the outline of both shoulders and upper arms are within the image

THERMAL IMAGE

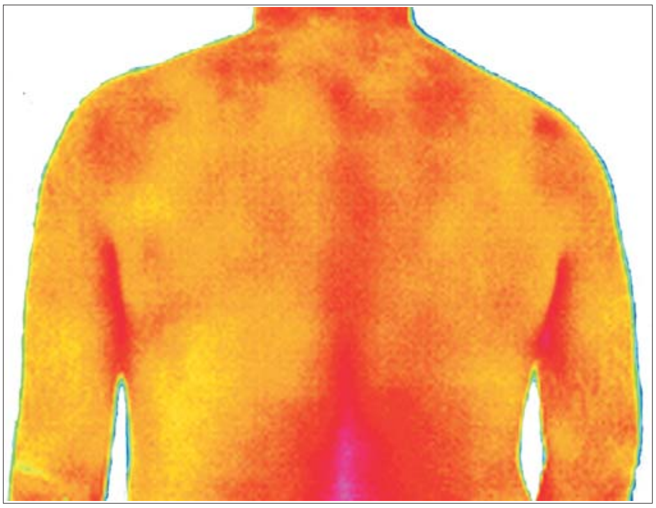

8. Right arm (anterior view); Code: RAA

upper edge of the image	wrist
lower edge of the image:	below the axillar fold
other condition	arm 90° abducted and elbow 90° bent, the outline of the of the deltoid muscle is within the image

THERMAL IMAGE

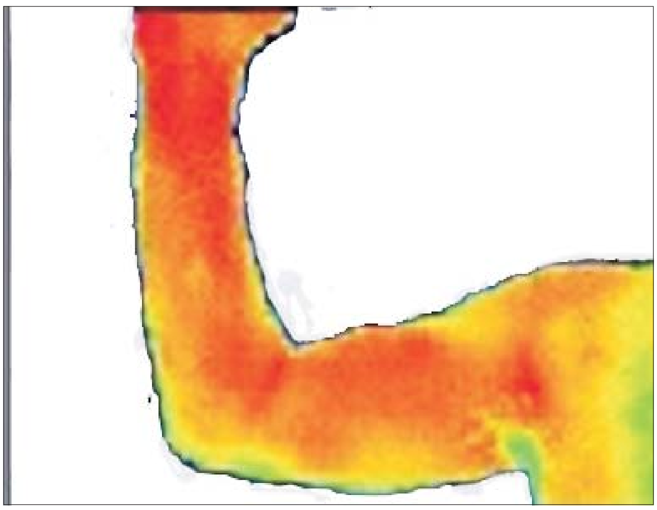

9. Right arm (dorsal view); Code: RAD

Upper edge of the image wrist
Lower edge of the image below the axillar fold
other condition arm 90° abducted and elbow 90° bent, the outline of the of the deltoid muscle is within the image

THERMAL IMAGE

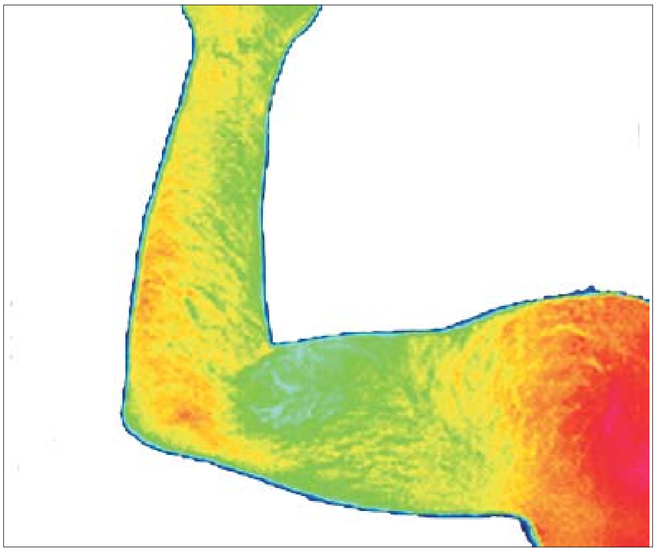

10. Left arm (anterior view); Code: LAA

upper edge of the image wrist
lower edge of the image below the axillar fold
other condition arm 90° abducted and elbow 90° bent, the outline of the of the deltoid muscle is within the image

THERMAL IMAGE

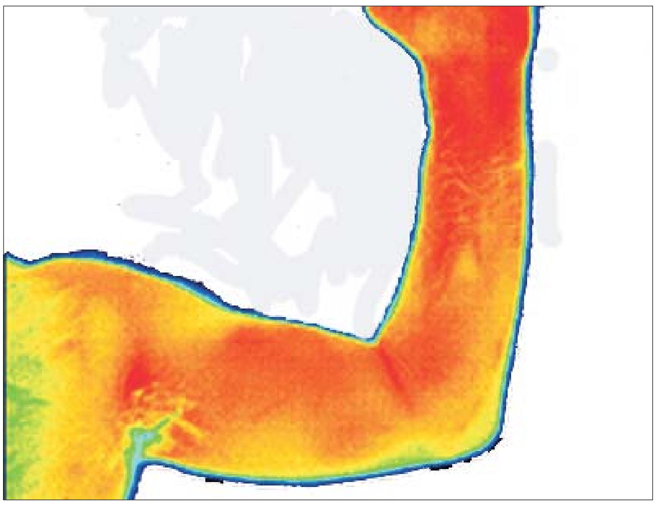

11. Left arm (dorsal view); Code: LAD

upper edge of the image wrist
lower edge of the image: below the axillar fold
other condition arm 90° abducted and elbow 90° bent, the outline of the of the deltoid muscle is within the image

THERMAL IMAGE

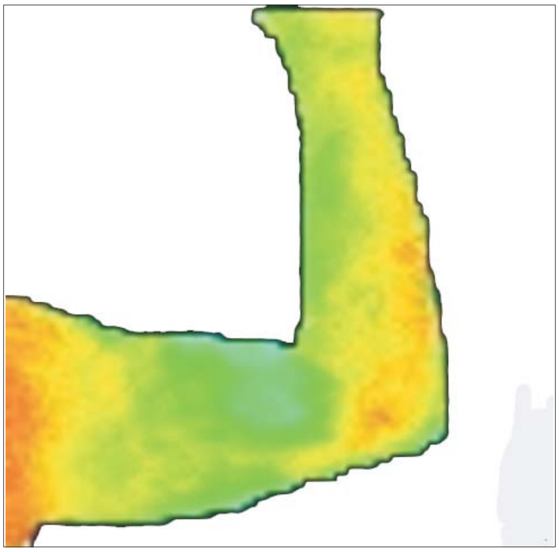

12. Both Hands (dorsal view); Code: BHD

upper edge of the image Wrist must be within the image
Left edge of the image Tip of the right little finger
Right edge of the image Tip of the right little finger
lower edge of the image tip of the middle finger
other condition middle fingers are parallel, thumbs do not touch

THERMAL IMAGE

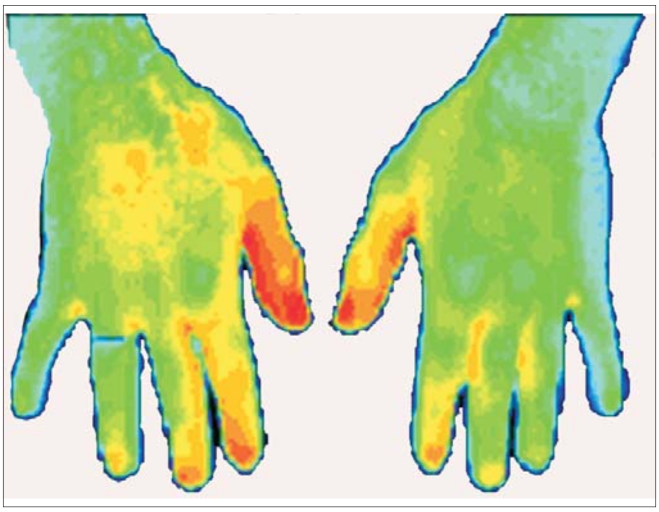

13. Abdomen; Code: ABD

upper edge of the image anterior fold of the axilla
lower edge of the image: lower end of the groin
other condition arms and legs slightly abducted

THERMAL IMAGE

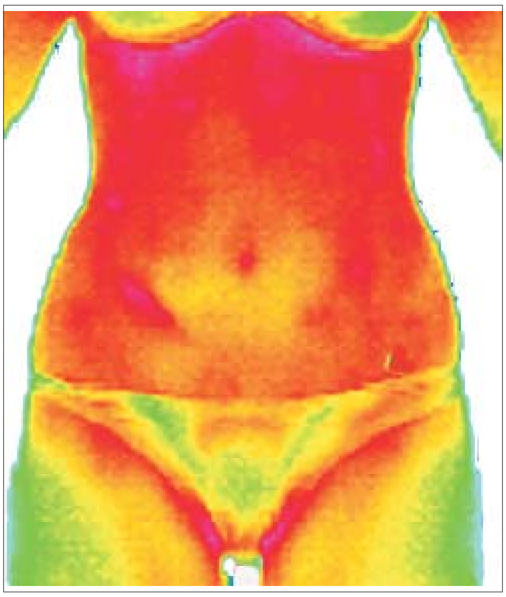

14. Lower Back; Code: LB

upper edge of the image posterior fold of the axilla
lower edge of the image: upper end of the natal cleft
other condition arms and legs slightly abducted

THERMAL IMAGE

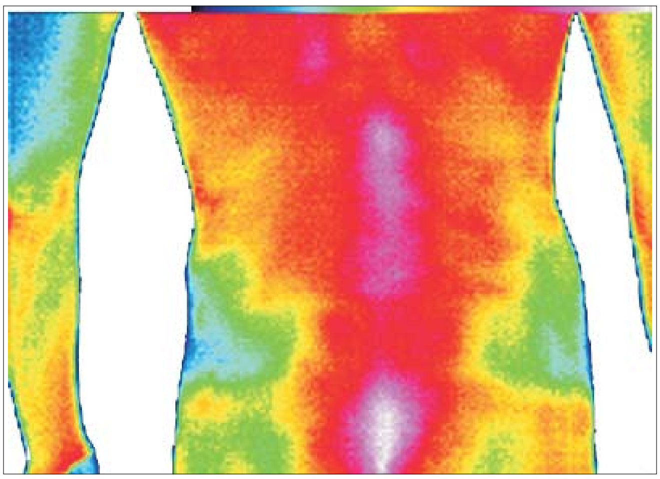

15. Thighs (anterior view); Code: TA

upper edge of the image line at the iliac crest
lower edge of the image: tip of the patella
other conditio*n* legs slightly abducted, feet parallel and the big toes point towards the camera

THERMAL IMAGE

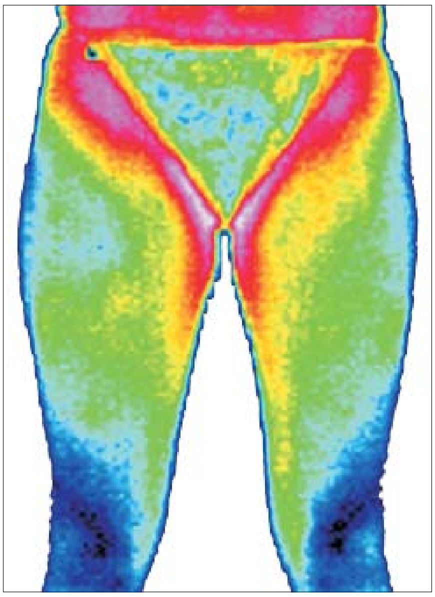

16. Thighs (dorsal view); Code: TD

upper edge of the image line at the crest
lower edge of the image head of fib ula
Other condition legs slightly abducted, feet parallel and the big toes point towards the camera

THERMAL IMAGE

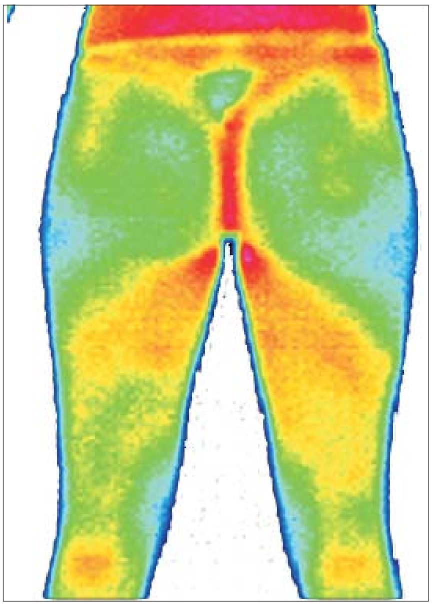

17 Leg , right (lateral view); Code: LRL

upper edge of the image iliac crest	
lower edge of the image: sole	
other condition hip and knee are approximately 90° bent, foot is placed on a chair, the total leg is in the sagittal plane of the body	

THERMAL IMAGE

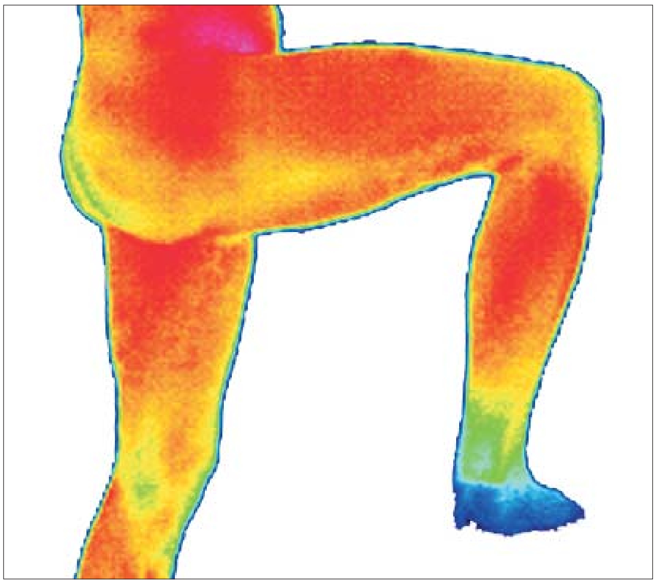

18. Leg, left (lateral view); Code: LLL

upper edge of the image iliac crest	
lower edge of the image: sole	
other condition hip and knee are approximately 90° bent, foot is placed on a chair, the total leg is in the sagittal plane of the body	

THERMAL IMAGE

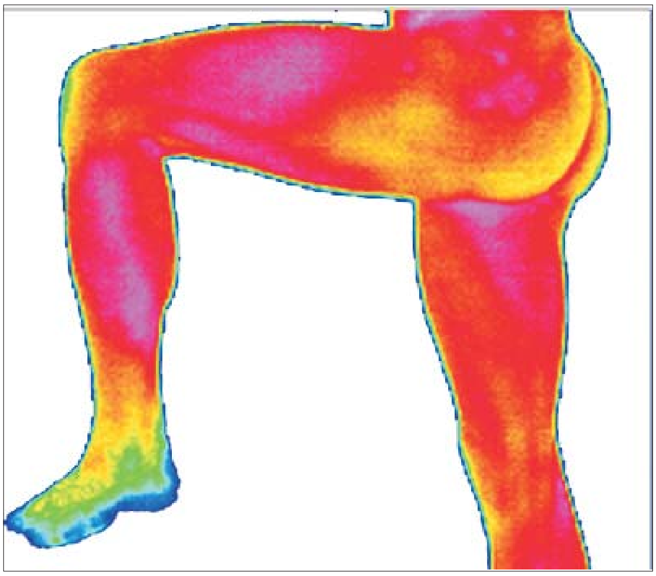

19. Lower Legs (anterior view); Code: LLA

upper edge of the image 1 inch above the rim of the patella	
lower edge of the image: soles	
other condition legs slightly abducted, feet parallel and the big toes point towards the camera	

THERMAL IMAGE

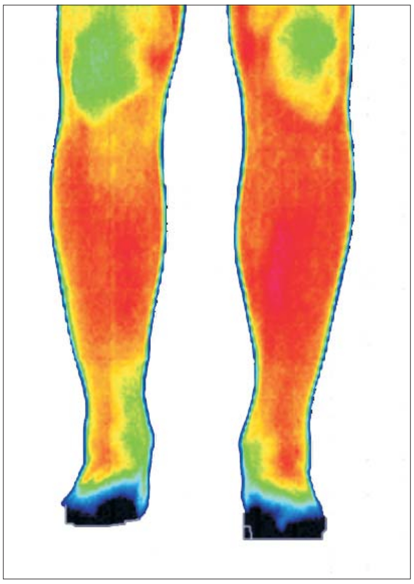

20. Lower Legs (dorsal view); Code: LLD

upper edge of the image 1 inch above the femoral condyli	
lower edge of the image: soles	
other condition legs slightly abducted, feet parallel and the big toes point towards the camera	

THERMAL IMAGE

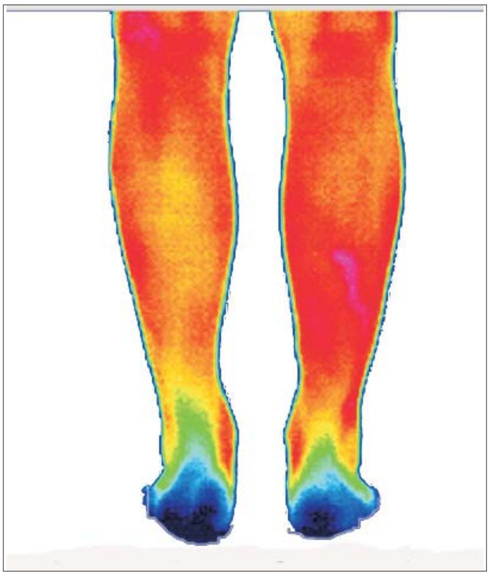

21. Both Knees (anterior view); Code: BKA

Upper edge of the image 1 inch above the femoral condyli
Lower edge of the image: soles
Other condition legs slightly abducted, feet parallel and the big toes point towards the camera

THERMAL IMAGE

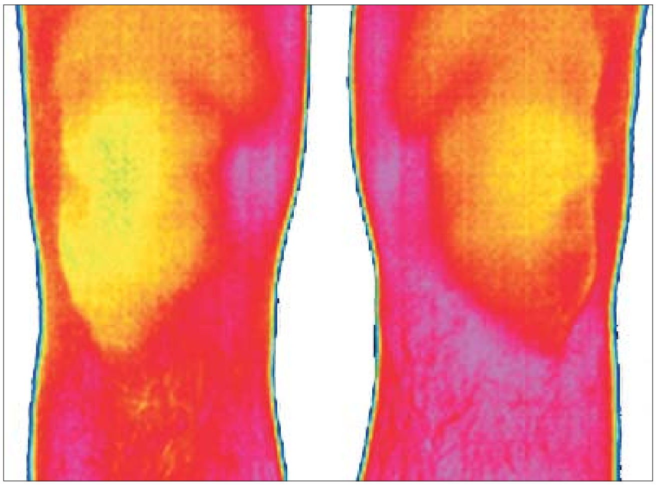

22. Both Ankles (anterior view); Code: BAA

Upper edge of the image 1 inch above the malleoli
Lower edge of the image: soles
Other condition legs slightly abducted, feet parallel and the big toes point towards the camera

THERMAL IMAGE

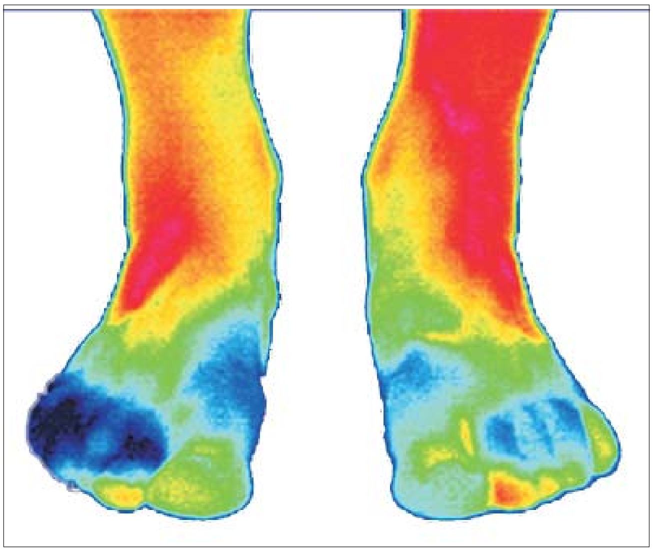

23. Dorsal Feet; Code: DF

Upper edge of the image Ankle
Lower edge of the image*:* tip of the great toe
other condition Subject sits on a chair, legs slightly abducted, feet parallel and the big toes point forwards Camera is in a rectangle position to the dorsal surface of the feet

THERMAL IMAGE

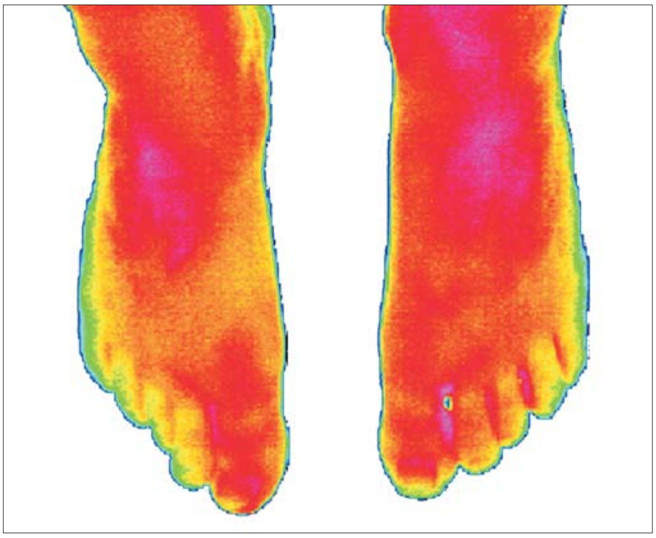

24. Plantar Feet; Code: PF

Upper edge of the image tip of the great toe
Lower edge of the image*:* heel
Other condition heels are placed on a chair, the angle between the lower leg and the foot is 90°, both feet are parallel

THERMAL IMAGE

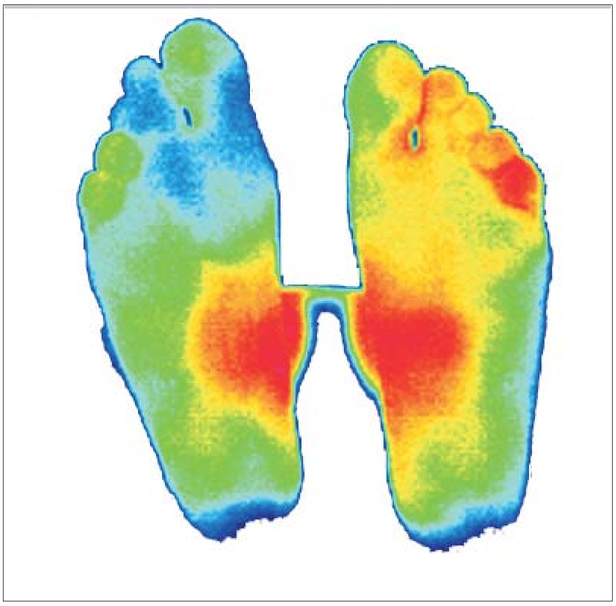

Regions of interest (ROI) A total of 90 ROIs is defined

View: Total body (anterior); Code: TBA

Number of ROIs: 1
Shape: polygon, following the outline of the body

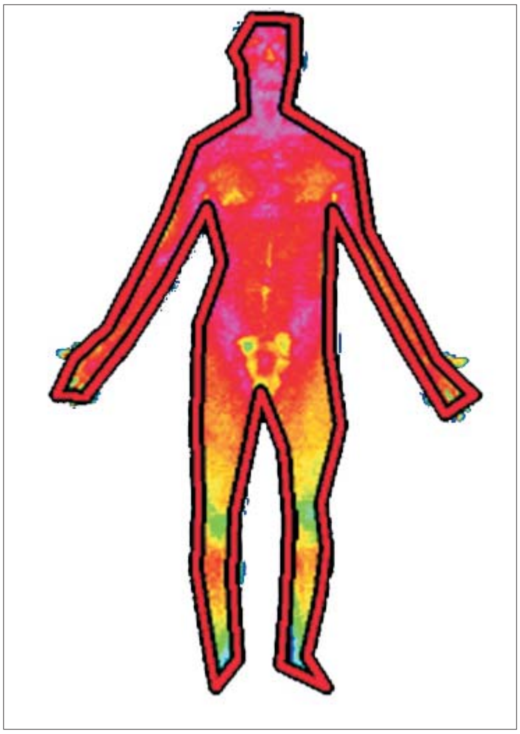

View: Total body (dorsal); Code: TBD

Number of ROIs: 1
Shape: polygon, following the outline of the body

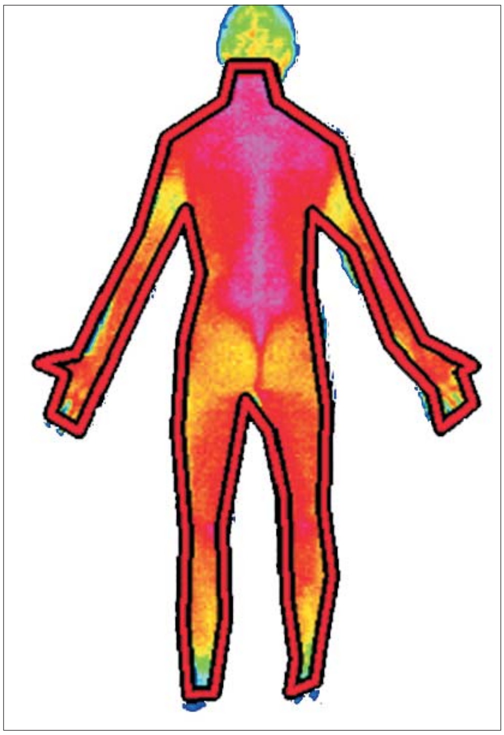

View: Total body (lateral);Code: TBL(eft)

Number of ROIs: 1
Shape: polygon, following the outline of the body

View: Total body (lateral);Code: TBR (right)

Number of ROIs: 1
Shape: polygon, following the outline of the body

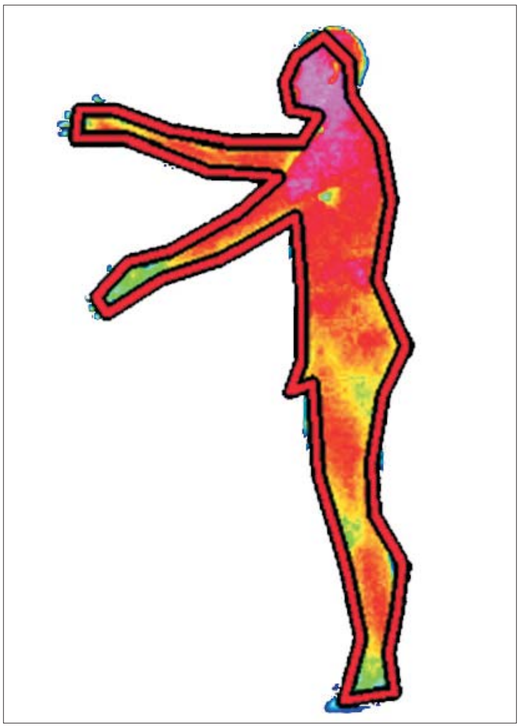

View: Face; Code: FA

Number of ROIs: 4
ROI 1: half of the face (red)
Shape: polygon
Outline of the face from the scalp to the chin, following the midline of the face
ROI 2: half of the face (blue)
Shape: polygon
Outline of the face from the scalp to the chin, following the midline of the face
ROI 3: half of the face (yellow)
Shape: rectangle
Lower edge: adjacent to the right eyebrow **Right upper corner**: adjacent to the hair line **Left upper corner:** adjacent to the midline of the face
ROI 4: half of the face (green)
Shape: rectangle
Lower edge: **Right upper corner**: adjacent to the midline of the face **Left upper corner:** adjacent to the left eyebrow

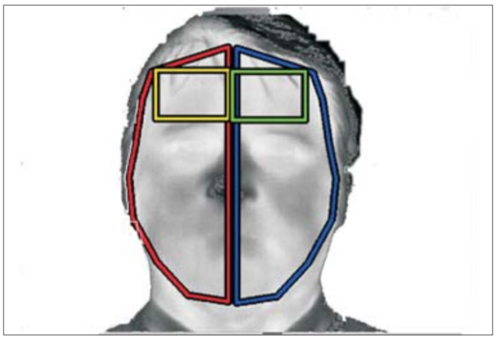

View: Neck: Code: ND

Number of ROIs: 2
ROI 1: half of the neck (red)
Shape:rectangle
Upper edge: adjacent to the hair line **Lower right corner**: adjacent to the junction of the outline of the trapeze muscle with the outline of the neck **Left edge:** adjacent to midline of the neck
ROI 2: half of the neck(blue)
Shape: rectangle
Upper edge: adjacent to the hair line **Right edge:** adjacent to midline of the neck **Lower left corner**: adjacent to the junction of the outline of the trapeze muscle with the outline of the neck

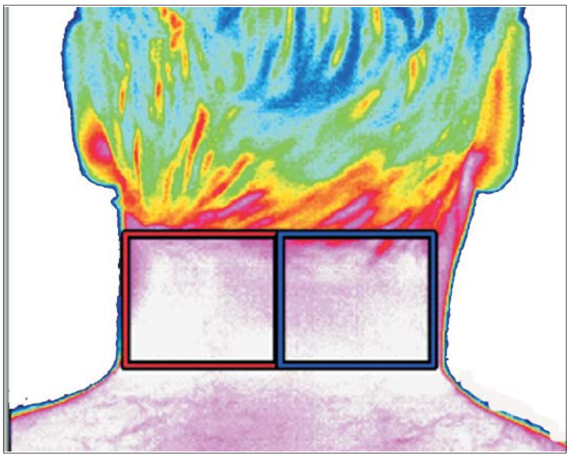

View: Chest; Code: CA

Number of ROIs: 4
ROI 1: right anterior shoulder joint (red)
Shape:circle
Outline of the circle is adjacent to the acromion and also to the anterior axillary fold
ROI 2: left anterior shoulder joint (blue)
Shape: Circle
Outline of the circle is adjacent to the acromion and also to the anterior axillary fold
ROI 3: half of the chest (yellow)
Shape: rectangle
Lower edge: aligned with the right elbow **Right upper corner**: adjacent to the acromion **Left upper corner:** adjacent to the midline of the chest
ROI 4: half of the chest (green)
Shape: rectangle
Lower edge: aligned with the left elbow **Right upper corner**: adjacent to the midline of the chest **Left upper corner:** adjacent to the acromion

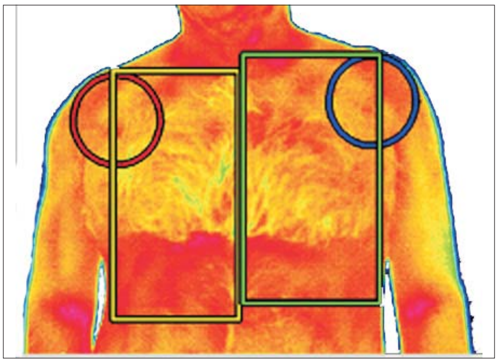

View: Upper Back: Code: UB

Number of ROIs: 4
ROI 1: left posterior shoulder joint (red)
Shape:circle
Outline of the circle is adjacent to the acromion and also to the posterior axillary fold
ROI 2: right anterior shoulder joint (blue)
Shape: Circle
Outline of the circle is adjacent to the acromion and also to the posterior axillary fold
ROI 3: half of the upper back (yellow)
Shape: rectangle
Lower edge: aligned with the left elbow **Right upper corner**: adjacent to the acromion **Left upper corner:** adjacent to the midline of the chest
ROI 4: half of the upper back (green)
Shape: rectangle
Lower edge: aligned with the right elbow **Right upper corner**: adjacent to the midline of the chest **Left upper corner:** adjacent to the acromion

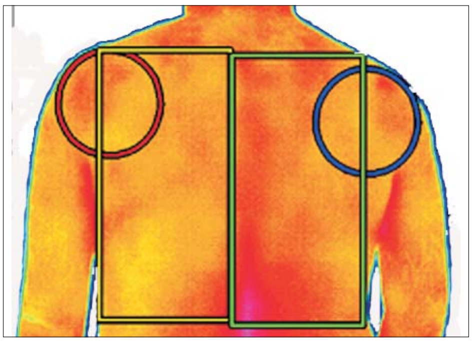

Right arm (anterior view); Code: RAA

Number of ROIs: 3
ROI 1: medial elbow (red)
Shape:circle
Outline of the circle is adjacent to the cubital fold and the lower edges of the elbow
ROI 2: anterior upper arm (blue)
Shape: trapezoid
Upper left corner: insertion of the deltoid muscle **Upper right corner**: cubital fold **Lower right corner:** tip of the elbow **Lower left corner:** axillary fold
ROI 3:anterior forearm (yellow)
Shape: trapezoid
Upper left corner: radial end of wrist **Upper right corner:** ulnar end of the wrist **Lower right corner:** tip of the elbow **Lower left corner:** cubital fold

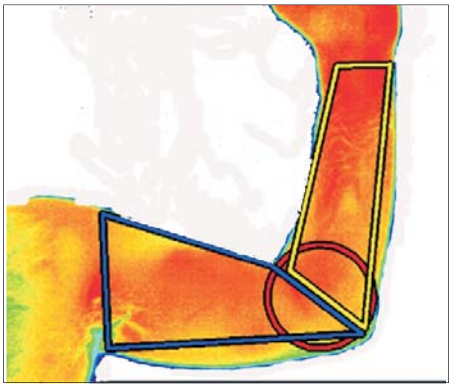

Right arm (dorsal view); Code: RAD

Number of ROIs: 3
ROI 1: lateral elbow (red)
Shape:circle
Outline of the circle is adjacent to the cubital fold and the lower edges of the elbow
ROI 2: posterior upper arm (blue)
Shape: trapezoid
Upper left corner: insertion of the deltoid muscle **Upper right corner:** cubital fold **Lower right corner:** tip of the elbow **Lower left corner:** axillary fold
ROI 3:posterior forearm (yellow)
Shape: trapezoid
Upper left corner: radial end of the wrist **Upper right corner:** ulnar end of the wrist **Lower right corner**: tip of the elbow **Lower left corner:** cubital fold

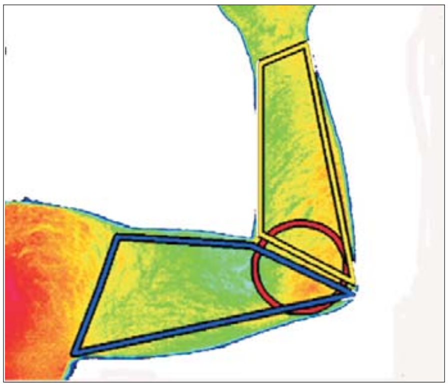

Left arm (anterior view); Code: LAA

Number of ROIs: 3
ROI 1: medial elbow (red)
Shape:circle
Outline of the circle is adjacent to the cubital fold and the lower edges of the elbow
ROI 2: anterior upper arm (blue)
Shape: trapezoid
Upper left corner: cubital fold **Upper right corner:** insertion of the deltoid muscle **Lower right corner:** axillary fold **Lower left corner**: tip of the elbow
ROI 3:anterior forearm (yellow)
Shape: trapezoid
Upper left corner: ulnar end of the wrist **Upper right corner:** radial end of the wrist **Lower right corner:** cubital fold **Lower left corner:** tip of the elbow

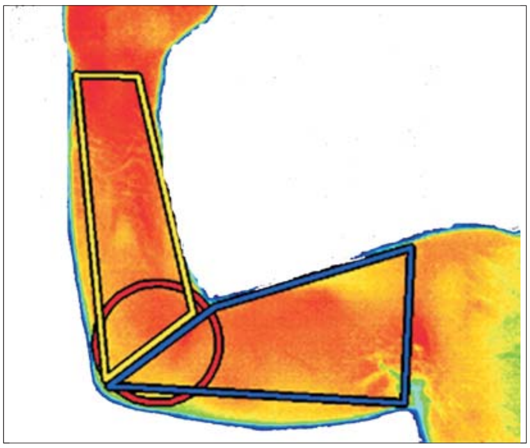

Left arm (posterior view); Code: LAD

Number of ROIs: 3
ROI 1: lateral elbow (red)
Shape:circle
Outline of the circle is adjacent to the cubital fold and the lower edges of the elbow
ROI 2: posterior upper arm (blue)
Shape: trapezoid
Upper left corner: cubital fold **Upper right corner:** insertion of the deltoid muscle **Lower right corner:** axillary fold **Lower left corner:** tip of elbow
ROI 3:posterior forearm (yellow)
Shape: trapezoid
Upper left corner: ulnar end of the wrist **Upper right corner:** radial end of the wrist **Lower right corner:** cubital fold **Lower left corner: tip of the elbow**

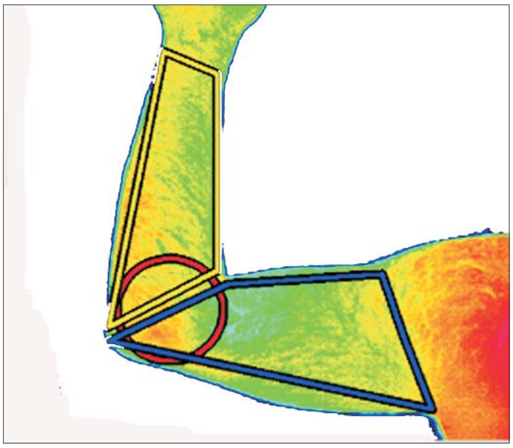

View: Both Hands (dorsal view); Code: BHD
Number of ROIs: 32, 1 over each wrist, 3 on each finger
Number of X-sections: 10, 1 on each finger

Wrist
ROI 1 right Wrist (red)
Shape: ellipse
Adjacent to the lateral edges of the wrist, proportion of both axes of the ellipse is approximately 1:3
ROI 2: left Wrist (blue)
Shape: ellipse
Adjacent to the lateral edges of the wrist, proportion of both axes of the ellipse is approximately 1:3

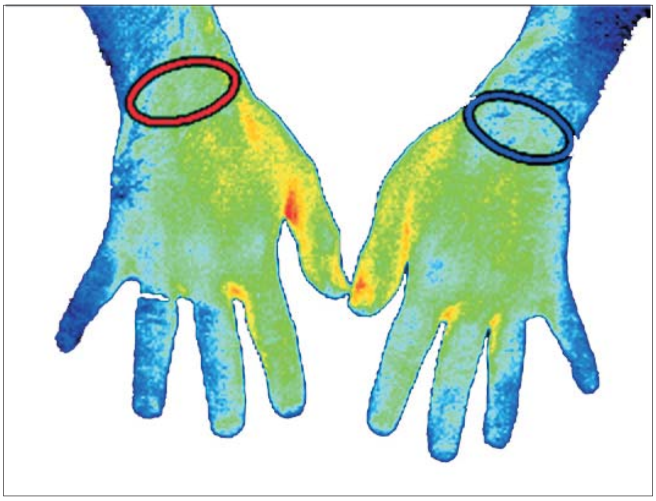

Right Thumb
ROI 1: interphalangeal joint (red)
Shape:circle
Outline of the circle is adjacent to the edges of the interphalangeal joint
ROI 2: metacarpophalangeal joint (blue)
Shape: circle
Outline of the circle is adjacent to the edges of the metacarpophalangeal joint
ROI 3:carpo-metacarpal joint (yellow)
Shape: circle
Outline of the circle is adjacent to the edges of the carpo-metacarpal joint
X-section (red)
In the midline of the thumb from the finger tip to the proximal end of the metacarpus

Left Thumb
ROI 1: interphalangeal joint (red)
Shape:circle
Outline of the circle is adjacent to the edges of the interphalangeal joint
ROI 2: metacarpophalangeal joint (blue)
Shape: circle
Outline of the circle is adjacent to the edges of the metacarpophalangeal joint
ROI 3:carpo-metacarpal joint (yellow)
Shape: circle
Outline of the circle is adjacent to the edges of the carpo-metacarpal joint
X-section (red)
In the midline of the thumb from the finger tip to the proximal end of the metacarpus

Right index finger
ROI 1: distal interphalangeal joint (red)
Shape: ellipse
Outline of the circle is adjacent to the finger tip and includes the proximal portion of the distal interphalangeal joint
ROI 2: proximal interphalangeal joint (blue)
Shape: circle
Outline of the circle is adjacent to the edges of the proximal interphalangeal joint
ROI 3:carpo-metacarpal joint (yellow)
Shape: circle
Outline of the circle is adjacent to the edges of the carpo-metacarpal joint
X-section (red)
In the midline of the index finger from the finger tip to the proximal end of the metacarpus

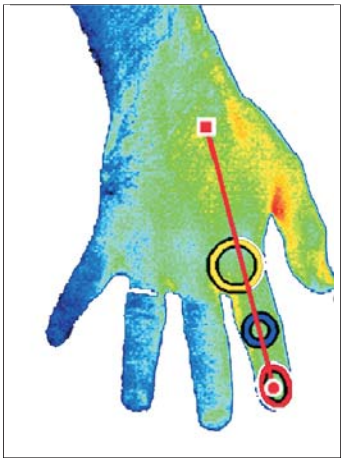

Left index finger
ROI 1: distal interphalangeal joint (red)
Shape: ellipse
Outline of the circle is adjacent to the finger tip and includes the proximal portion of the distal interphalangeal joint
ROI 2: proximal interphalangeal joint (blue)
Shape: circle
Outline of the circle is adjacent to the edges of the proximal interphalangeal joint
ROI 3:carpo-metacarpal joint (yellow)
Shape: circle
Outline of the circle is adjacent to the edges of the carpo-metacarpal joint
X-section (red)
In the midline of the index finger from the finger tip to the proximal end of the metacarpus

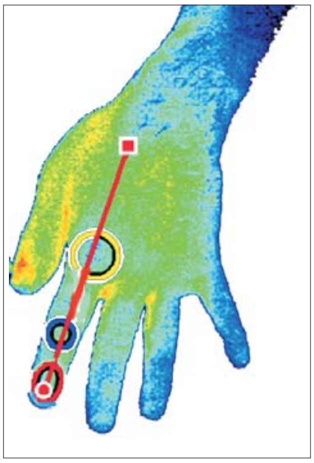

Right middle finger
ROI 1: distal interphalangeal joint (red)
Shape: ellipse
Outline of the circle is adjacent to the finger tip and includes the proximal portion of the distal interphalangeal joint
ROI 2: proximal interphalangeal joint (blue)
Shape: circle
Outline of the circle is adjacent to the edges of the proximal interphalangeal joint
ROI 3:carpo-metacarpal joint (yellow)
Shape: circle
Outline of the circle is adjacent to the edges of the carpo-metacarpal joint
X-section (red)
In the midline of the middle finger from the finger tip to the proximal end of the metacarpus

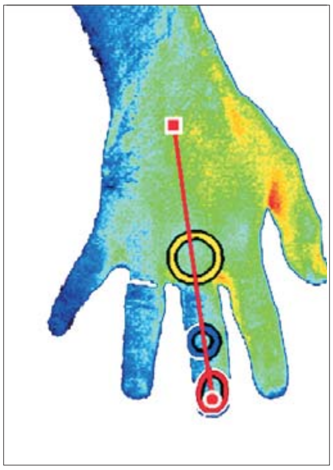

Left middle finger
ROI 1: distal interphalangeal joint (red)
Shape: ellipse
Outline of the circle is adjacent to the finger tip and includes the proximal portion of the distal interphalangeal joint
ROI 2: proximal interphalangeal joint (blue)
Shape: circle
Outline of the circle is adjacent to the edges of the proximal interphalangeal joint
ROI 3:carpo-metacarpal joint (yellow)
Shape: circle
Outline of the circle is adjacent to the edges of the carpo-metacarpal joint
X-section (red)
In the midline of the middle finger from the finger tip to the proximal end of the metacarpus

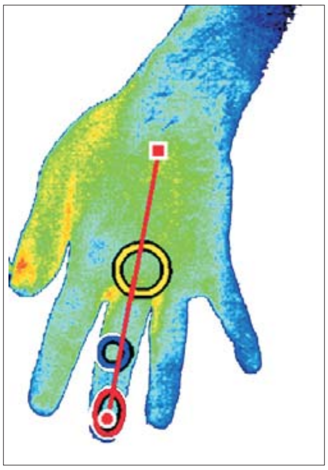

Right ring finger
ROI 1: distal interphalangeal joint (red)
Shape: ellipse
Outline of the circle is adjacent to the finger tip and includes the proximal portion of the distal interphalangeal joint
ROI 2: proximal interphalangeal joint (blue)
Shape: circle
Outline of the circle is adjacent to the edges of the proximal interphalangeal joint
ROI 3:carpo-metacarpal joint (yellow)
Shape: circle
Outline of the circle is adjacent to the edges of the carpo-metacarpal joint
X-section (red)
In the midline of the ring finger from the finger tip to the proximal end of the metacarpus

Left ring finger
ROI 1: distal interphalangeal joint (red)
Shape: ellipse
Outline of the circle is adjacent to the finger tip and includes the proximal portion of the distal interphalangeal joint
ROI 2: proximal interphalangeal joint (blue)
Shape: circle
Outline of the circle is adjacent to the edges of the proximal interphalangeal joint
ROI 3:carpo-metacarpal joint (yellow)
Shape: circle
Outline of the circle is adjacent to the edges of the carpo-metacarpal joint
X-section (red)
In the midline of the ring finger from the finger tip to the proximal end of the metacarpus

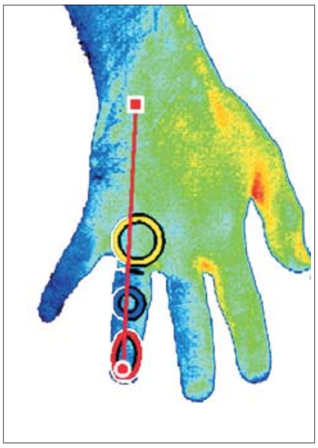

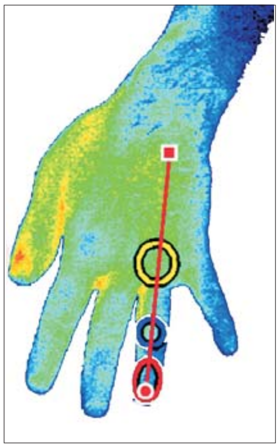

Right little finger
ROI 1: distal interphalangeal joint (red)
Shape: ellipse
Outline of the circle is adjacent to the finger tip and includes the proximal portion of the distal interphalangeal joint
ROI 2: proximal interphalangeal joint (blue)
Shape: circle
Outline of the circle is adjacent to the edges of the proximal interphalangeal joint
ROI 3:carpo-metacarpal joint (yellow)
Shape: circle
Outline of the circle is adjacent to the edges of the carpo-metacarpal joint
X-section (red)
In the midline of the little finger from the finger tip to the proximal end of the metacarpus

Left little finger
ROI 1: distal interphalangeal joint (red)
Shape:circle
Outline of the circle is adjacent to the finger tip and includes the proximal portion of the distal interphalangeal joint
ROI 2: proximal interphalangeal joint (blue)
Shape: circle
Outline of the circle is adjacent to the edges of the proximal interphalangeal joint
ROI 3:carpo-metacarpal joint (yellow)
Shape: circle
Outline of the circle is adjacent to the edges of the carpo-metacarpal joint
X-section (red)
In the midline of the little finger from the finger tip to the proximal end of the metacarpus

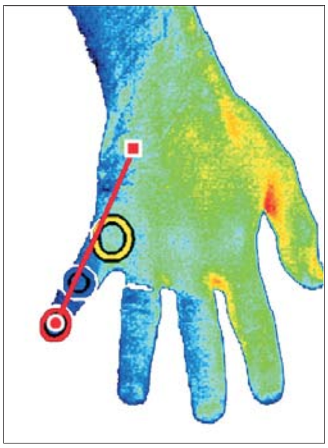

View: Abdomen; Code:ABD

Number of ROIs: 2
ROI 1: half of the abdomen (red)
Shape: rectangle
Upper left corner: aligned with the right elbow **Upper right corner:** at the midline of the body **Lower right corner:** lower end of the right groin **Lower left corner:** upper end of the right groin
ROI 2: half of the abdomen(blue)
Shape: rectangle
Upper left corner: at the midline of the body **Upper right corner:** aligned with the left elbow **Lower right corner:** upper end of the left groin **Lower left corner:** lower end of the left groin

Thighs (anterior view); Code: TA

Number of ROIs: 2
ROI 1: right thigh (red)
Shape: polygon, following the outline of the thigh
Upper left corner: upper end of the groin **Upper right corner:** lower end of the groin **Lower edge:** horizontal line aligned with the rim of the patella
ROI 2: left thigh (blue)
Shape: polygon, following the outline of the thigh
Upper left corner: lower end of the groin **Upper right corner:** upper end of the groin **Lower edge:** horizontal line aligned with the rim of the patella

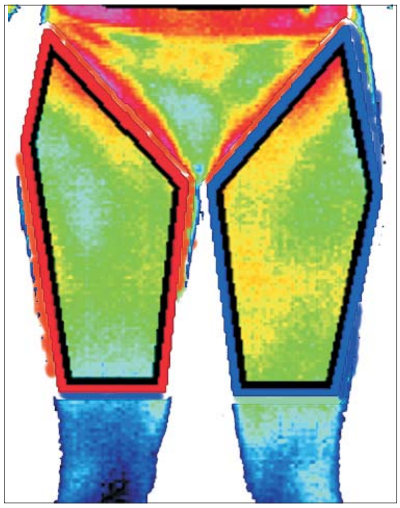

View: Lower Back, Code: LB

Number of ROIs: 2
ROI 1: half of the lower back (red)
Shape: triangle
Upper corner: at the midline of the body **Left corner:** adjacent to the natal cleft **Right corner:**aligned with the natal cleft at the left side of the body
ROI 2: half of the lower back (blue)
Shape: rectangle
Upper corner: at the midline of the body **Left corner:** aligned with the natal cleft at the left side of the body **Right corner**: adjacent to the natal cleft

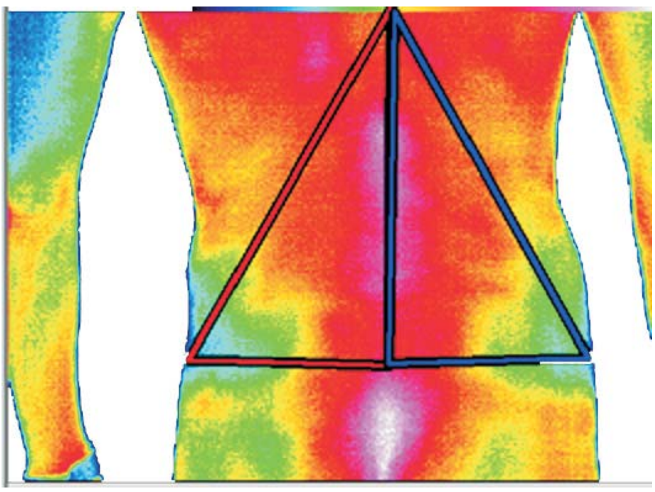

16. Thighs (dorsal view); Code: TD

Number of ROIs: 2
ROI 1: left thigh (red)
Shape: polygon, following the outline of the thigh
Upper edge: horizontal line aligned with the gluteal fold **Lower edge:** horizontal line aligned with the tip of the fibula
ROI 2: right thigh (blue)
Shape: polygon, following the outline of the thigh
Upper edge: horizontal line aligned with the gluteal fold **Lower edge:** horizontal line aligned with the tip of the fibula

Leg , right (lateral view); Code: LRL

Number of ROIs: 3
ROI 1: medial knee (red)
Shape:circle
Outline of the circle is adjacent to outline of the patella and the popliteal cubital fold
ROI 2: lateral hip (blue)
Shape: circle
Outline of the circle is adjacent to outline of the nates
ROI 3:lateral ankle (yellow)
Shape: circle
Outline of the circle is within the outlines of the ankle region

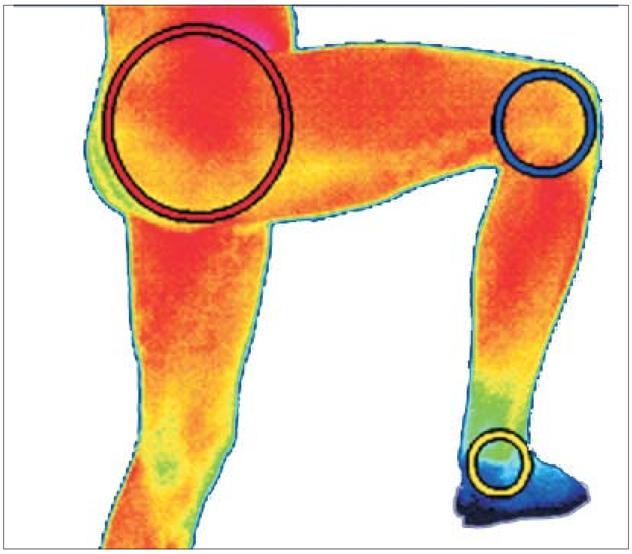

Lower Legs (anterior view); Code: LLA

Number of ROIs: 2
ROI 1: right lower leg (red)
Shape: polygon, following the outline of the lower leg
Upper edge : horizontal line aligned with the tip of the fibula
Lower edge: horizontal line at the minimal width of the lower leg
ROI 2: left lower leg (blue)
Shape: polygon, following the outline of the lower leg
Upper edge : horizontal line aligned with the tip of the fibula
Lower edge: horizontal line at the minimal width of the lower leg

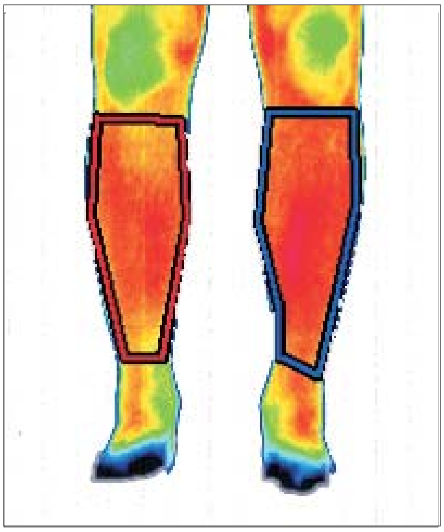

Leg, left (lateral view); Code: LLL

Number of ROIs: 3
ROI 1: medial knee (red)
Shape:circle
Outline of the circle is adjacent to outline of the patella and the popliteal cubital fold
ROI 2: lateral hip (blue)
Shape: circle
Outline of the circle is adjacent to outline of the nates
ROI 3:lateral ankle (yellow)
Shape: circle
Outline of the circle is within the outlines of the ankle region

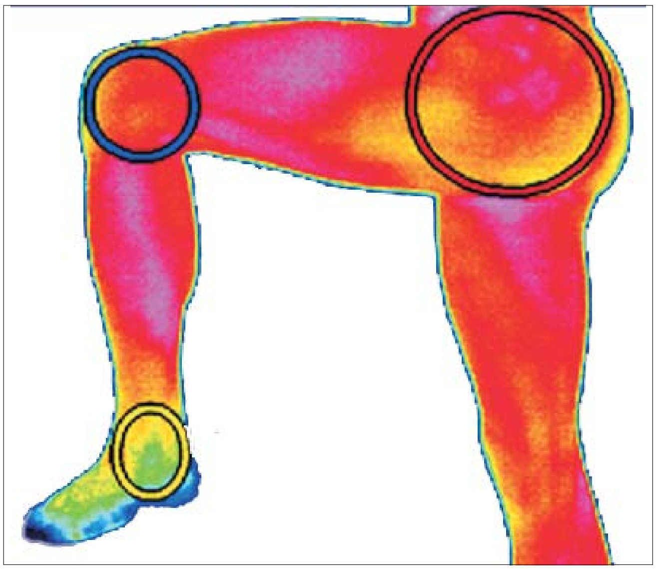

Lower Legs (dorsal view); Code: LLD

Number of ROIs: 2
ROI 1: left lower leg (red)
Shape: polygon, following the outline of the lower leg
Upper edge : horizontal line aligned with the tip of the fibula
Lower edge: horizontal line at the minimal width of the lower leg
ROI 2: right lower leg (blue)
Shape: polygon, following the outline of the lower leg
Upper edge : horizontal line aligned with the tip of the fibula
Lower edge: horizontal line at the minimal width of the lower leg

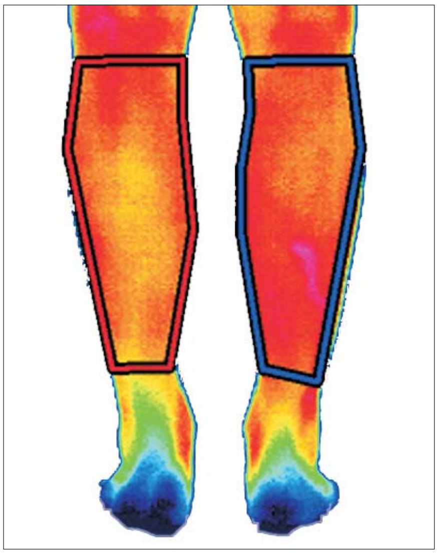

Both Knees (anterior view); Code: BKA

Number of ROIs: 2	
ROI 1: right knee (red)	
Shape: polygon following the outline of the knee	
Upper edge : horizontal line approximately 1 inch above the rim of the patella **Lower edge:** horizontal line aligned with the tip of the fibula	
ROI 2: left knee (blue)	
Shape: polygon following the outline of the knee	
Upper edge : horizontal line approximately 1 inch above the rim of the patella **Lower edge:** horizontal line aligned with the tip of the fibula	

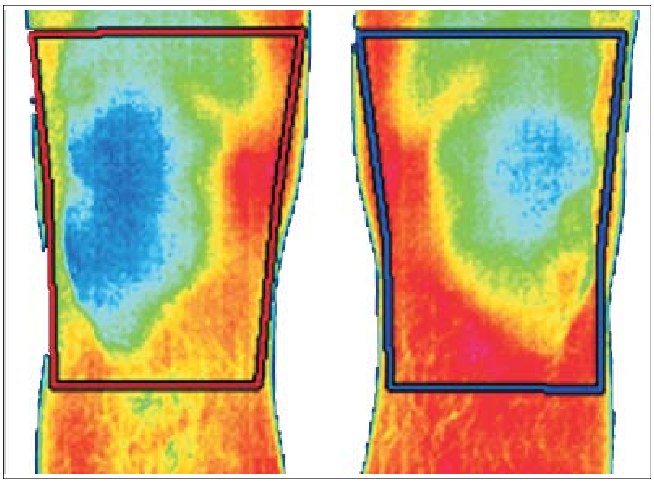

Both Ankles (anterior view); Code: BAA

Number of ROIs: 2	
ROI 1: right ankle (red)	
Shape: square rectangle	
Upper edge : aligned with the tip of medial malleolus **Lower edge:** aligned with the tip of the naviculare bone	
ROI 2: left ankle (blue)	
Shape: square rectangle	
Upper edge : aligned with the tip of medial malleolus **Lower edge:** aligned with the tip of the naviculare bone	

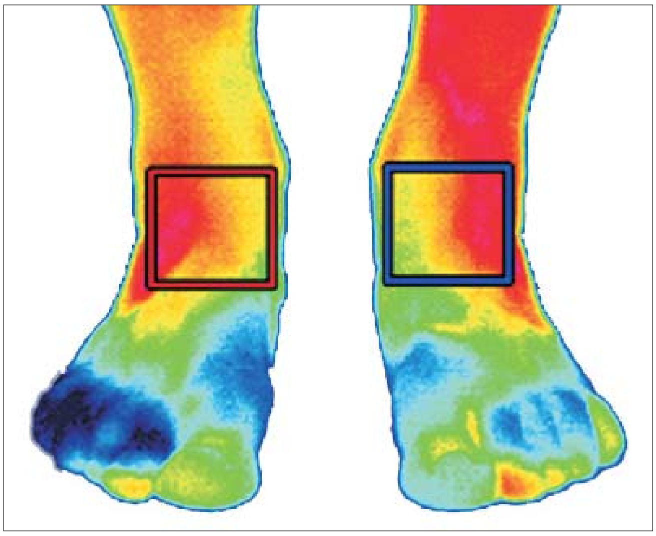

Dorsal Feet; Code: DF

Number of ROIs: 2	
ROI 1: right foot (red)	
Shape: polygon, following the outline of the foot	
Upper edge : horizontal line aligned with the tip of the naviculare	
ROI 2: left ankle (blue)	
Shape: square rectangle	
Shape: polygon, following the outline of the foot	
Upper edge : horizontal line aligned with the tip of the naviculare	

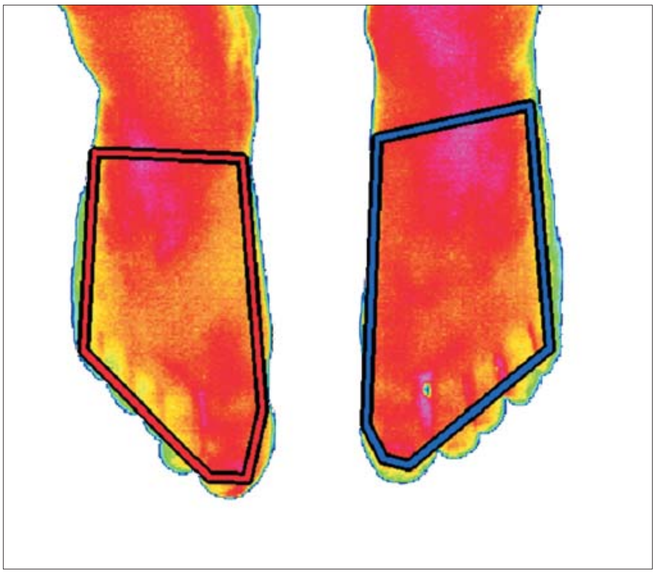

Plantar Feet; Code: PF

Number of ROIs: 2	
ROI 1: right sole (red)	
Shape: polygon, following the outline of the foot	
ROI 2: left sole (blue)	
Shape: polygon, following the outline of the foot	

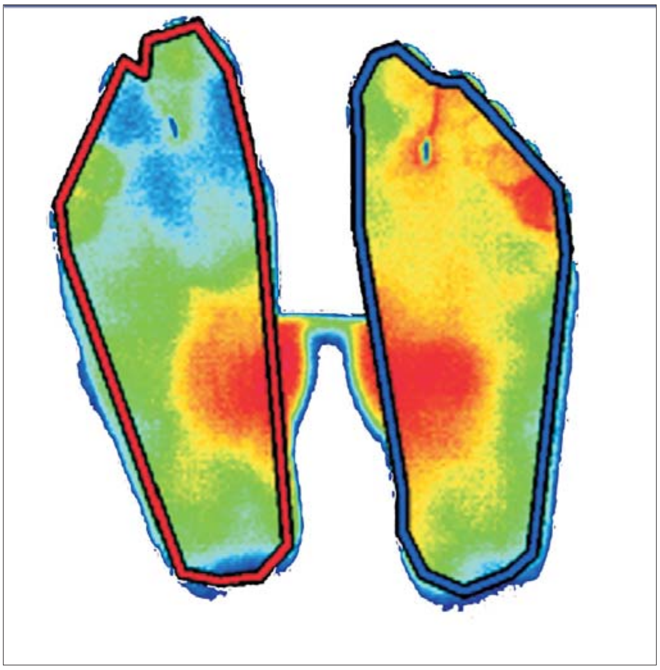

The Effect of Temperature and Time Using Repeated Immersion on the Habituation of Pain Thresholds in Healthy Subjects

M. J. Fischer [1], A. Khani [1], C.E. Gokpinar [1], E. Strueber [1], C. Gutenbrunner[1], M.Bernateck [2]

1 Department of Physical and Rehabilitation Medicine, Hannover Medical School, Hanover, Germany,

2 Department of Anesthesiology, Pain Clinic, Hanover Medical School, Hanover, Germany

SUMMARY

The habituation response to repeated cold-water immersion of parts of the extremities results in an increase of pain threshold elicited by pressure or hot and cold stimuli. 17 healthy male subjects immersed the forearms in 4 degree C water for 1 minute, followed by an interval of 1 minute, repeating the process 10 times. We measured skin temperature, pressure and temperature induced pain threshold, and cardiovascular parameters. Using the data obtained combined with a previous study, we found the pain threshold doubled over a wide temperature range. The time needed to achieve the same elevation of pain threshold was longer for higher temperatures. Our results suggest that many independent peripheral mechanisms may contribute to the habituation.

KEY WORDS: habituation, pain threshold, blood pressure, autonomic nerve system

DER EINFLUSS VON TEMPERATUR UND DAUER WIEDERHOLTER TAUCHBÄDER AUF DIE ANPASSUNG DER SCHMERZSCHWELLE GESUNDER PERSONEN

Die Habituationsantwort auf wiederholte Kaltwasser-Tauchbäder von Teilen der Extremitäten bedingt eine Erhöhung der Schmerzschwelle, die durch Druck oder Temperaturreize ausgelöst wird. 17 gesunde männliche Personen tauchten ihre Unterarme 1 Minute lang in Wasser von 4°C und wiederholten dies nach einer Pause von 1 Minute insgesamt 10 Mal. Die Hauttemperatur, die Schmerzschwelle für Druck und Temperaturreize und kardiovaskuläre Parameter wurden gemessen. Die Daten dieser und einer früheren Studie zeigten, dass sich die Schmerzschwellen über einen weiten Temperaturbereich um das Doppelte erhöhten. Um einen gleichartigen Effekt bei hohen Temperaturen zu erzielen, war mehr Zeit nötig. Unsere Ergebnisse stützen die Amsicht, dass unterschiedliche, voneinander unabhängige, periphere Mechanismen zur Habituation beitragen .

Schlüsselwörter: Habituation, Schmerzschwelle, Blutdruck, autonomes Nervensystem

Thermology international 2008, 18: 145-150

Introduction

The cold pressor test (CPT), in which a part of an extremity, such as the hand or forearm, is immersed into ice water (1-5°C) for a few minutes, is well known for its evocation of a vascular autonomic response in normal subjects [1,2]. Although a sustained blood pressure response is usually observed [3], there is considerable individual variability in regard to the heart rate response, which may increase or decrease [2].

Adaptation to cold water, including the CPT is common, although the magnitude of the effect depends on age, gender, and hormonal factors in women [4,5,6]. It is generally believed that separate nociceptive mechanisms may be responsible since Polianskis et al. [7] found that tolerance to tonic painful pressure and cold stimulation was specific to stimulus modality, and research in paraplegics indicates the presence of independent thoracic spinal mechanism [8]. Tamura and An [9] have also suggested that concurrent rises in core temperature that accompany local cooling of affected body areas might also be responsible for the decreased sensation at the cooling site.

When the CPT is repeated, a habituation or adaptation effect is manifested in response to the cold, which results in lower pain thresholds, although its magnitude depends on the interval of time between exposure to the cold stimulus, and usually disappears within an hour [5]. In a previous series of experiments, we investigated the habituation, which we termed the cold pressor response, in healthy subjects by immersing their whole forearms in a 4°C ice bath with intervals of 5 and 15 minutes between immersions, and examining the pressure pain threshold [10]. In this study, we wished to shorten the interval to 1 minute and to compare the results with the previous investigation.

Materials and Methods

Subjects

Seventeen healthy male subjects were enrolled in the study. Exclusion criteria included severe ongoing pain, circulatory disorders, cardiac problems, hypertension, fibromyalgia, neurological diseases, acute inflammatory conditions, wounds and systemic use of any pharmacological agents that would interfere with the protocol.

Study protocols

The study design was a crossover in which subjects were randomized by a statistician to one of 2 conditions, with the second condition performed after a 72-hour washout period. Patients gave written consent to participate in the study. The study was conducted in accordance with the ethical principles of the Declaration of Helsinki with the Edinburgh revision and according to current Good Clinical Practice guidelines and was approved by the local Ethics Committee.

Subjects were seated for 5 min and informed about the procedures. No attempt was made to cognitively influence the subjects regarding expectations or outcomes. After pulse and blood pressure measurements, pressure pain thresholds (PPTs) were assessed by pressure algometry at the processus styloideus radii. The pressure algometry apparatus (Model PTH, PDT 20100, Germany) used in the study applied approximately 40-60 kPa/s/cm², and the diameter of contact with the skin was approximately 1 cm. The temperature of the forearm skin was measured before and after the immersions using the Thermo Check M, a non- contact based infrared thermometer (Steinel, Germany) that operates via an infrared sensor; the probe was directed to the forearm at a distance of 5 cm. With spectral compensation, the achieved accuracy was ± 0.3°C. Prior to experimental use, calibration was performed for the necessary temperature range (10°C-42°C). The absolute accuracy after calibration was ± 0.3°C and the relative accuracy ± 0.1°C. The emissivity (epsilon) was adjusted to 0.97 according to the manufacturer´s recommendations for skin temperature measurements; the response time was < 1 second. Forearm skin temperature, cardiovascular parameters and pressure pain thresholds were measured after each immersion.

Hot and cold pain thresholds were determined using a computerized contact thermode Thermotest (Somedic A/B, Stockholm, Sweden) [11]. This device is capable of heating or cooling the skin, and consists of semiconductor junctions that produce a temperature gradient between the upper and lower stimulator surfaces produced by the passage of an electric current, thereby eliciting a cooling or heating effect. It is assumed that A-delta fibres mediate cold sensations, and most likely C-fibres mediate cold pain in humans [13]. All thresholds were assessed using a 2.5 x 5.0 cm thermode. The heat pain threshold was the lowest temperature perceived as painful obtained by starting at 32°C and increasing the thermode temperature to 52°C with a rate of change of 1°C sec^{-1}. Similarly, the cold pain temperature was then obtained by starting at 32°C and decreasing the temperature. Subjects were instructed to react to the first trace of pain by pressing a button connected to the device, which recorded the threshold. All thermal thresholds were determined as the average of 5 trials performed at 5 sec intervals. Measurements were made at baseline, and at the conclusion of each intervention for each subject.

All study parameters were measured with the forearm in air at room temperature. After obtaining baseline measurements, the arm was adducted and the elbow flexed at an angle of 90°, and the whole dominant forearm immersed in a water (city tap water) bath that was thermoneutral (36°C) (condition 1), or contained ice cubes (4°C) for 1 minute. Ten serial immersions were conducted for each condition with the immersion lasting 1 minute followed by a resting period in air of 1 minute while measurements were performed.

Statistical analysis

SPSS (SPSS, Chicago IL, version 15) was used for statistical analysis. Quantitative data are presented as mean values and standard deviations, and changes within groups or between groups were tested for statistical significance by ANOVA (t tests, simple or two correlated samples) where relevant. While a general significance level of 0.05 was chosen, with all tests performed as 2-sided, in the case of multiple t tests, a Holm sequential Bonferroni calculation was made to determine the statistical significance required for each measurement.

Results

The mean age of the subjects was 24.9 (3.76) years with a range of 18 to 35 years. In contrast to condition 1, the pressure pain threshold in condition 2 steadily rose throughout the experiment (Figure 1) from a baseline value of 5.89 Pa to 9.42 Pa, an increase of 60%. By comparison, the change (increase) in condition 1 was only 0.13 Pa. The difference between baseline and at each subsequent point for condition 2 was statistically significant ($p < 0.0005$).

For condition 1, the change in hot pain threshold between baseline and the conclusion of the experiment was minimal (0.21°C), whereas it was significantly higher for condition 2 (5.59°C, $p < 0.0005$) (Figure 2). Similar results were obtained with the cold pain threshold in which the change was also minimal for condition 1 (a nonsignificant drop of

Figure 1:
Pressure pain threshold before and following immersion of forearms in thermoneutral condition water and cold water (4ºC). Only a sampling of the results is presented to improve clarification of presentation.
Horizontal bars represent standard deviations.

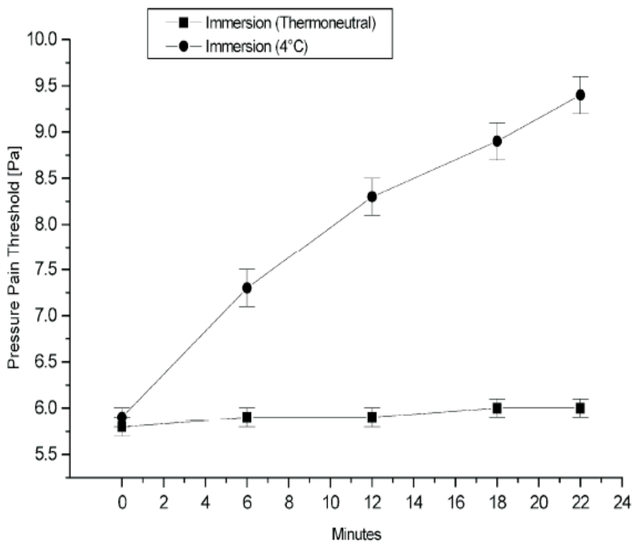

Fig ure 2
Mean hot pain threshold before and after immersion in thermoneutral condition water and cold water (4ºC). Horizontal bars represent standard error of the mean.

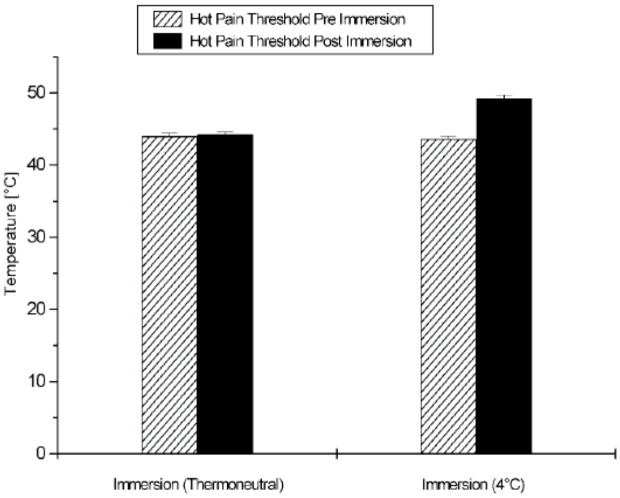

Figure 3
Mean cold pain threshold before and after immersion in thermoneutral condition water and cold water (4ºC). Horizontal bars represent standard error of the mean.

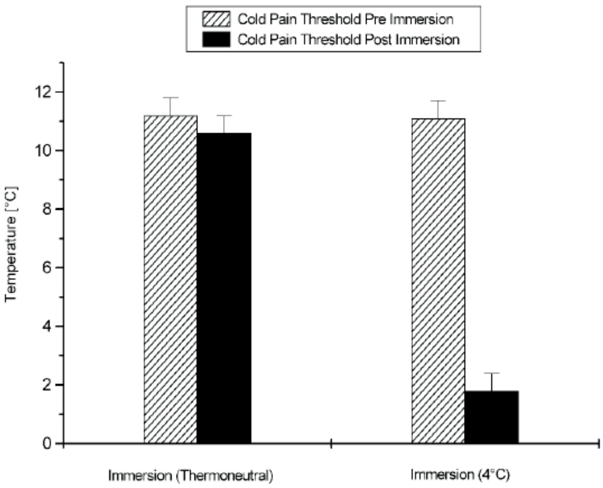

0.55°C) but large for condition 2 (drop of 9.29°C, $p < 0.0005$) (Figure 3).

In the case of systolic blood pressure, there was an immediate rise of approximately 14 mm Hg in condition 1 following the first immersion, which maintained with some variation throughout the experiment (Figure 4A). This increase was minimal for condition 1. Although the differences between baseline and various points during the experiment for condition 2 or between matched points for conditions 1 and 2 were in a few instances significant after the Bonferroni correction, overall, the differences should not be regarded as significant. A similar pattern was observed for the diastolic blood pressure except that there was considerably more variation and the overall differences between condition 1 and 2 were smaller (Figure 4B). In the case of

Figure 4
Changes in cardiovascular parameters before and following immersion of forearms in thermoneutral condition water and cold water (4ºC).
A: systolic blood pressure;
B: diastolic blood pressure;
C: heart rate.
Horizontal bars represent standard error of the mean.

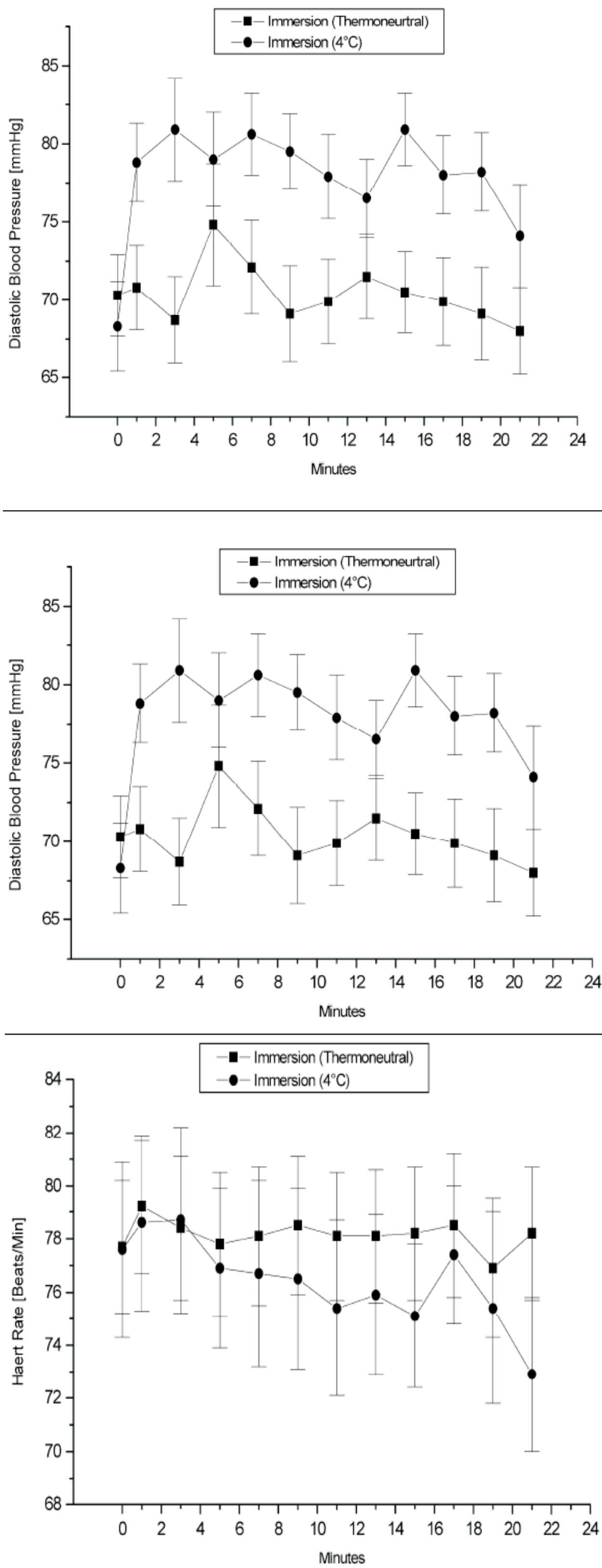

heart rate, a gradual non-significant difference between conditions 1 and 2 emerged as the experiment progressed, with the subjects in condition 2 experiencing a lower heart rate (Figure 4C).

The difference in forearm skin temperatures between conditions 1 and 2 was significant through the experiment ($p < .0005$) with the temperature initially dropping 14.2°C after the first immersion and gradually lowering with more immersions, until the maximum difference was 21.7°C (Figure 5).

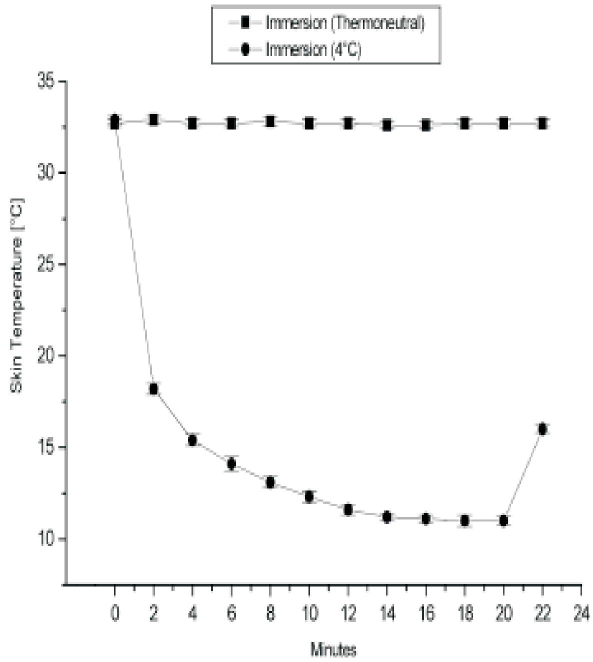

Figure 5
Fig 5: Change in forearm skin temperature before and after immersion in thermoneutral condition water and cold water (4ºC). Horizontal bars represent standard error of the mean.

Correlations were also plotted using mean values between surface temperature and pressure pain threshold for this study and incorporating data from the study of Kalpakcioglu et al. [10] (Figure 6), which showed that similar pain thresholds could be reached in the temperature range of 12°C-20°C. Another plot of time versus pressure pain threshold data from this study and data from the study of Kalpakcioglu et al. [10] (Figure 7) showed that lower temperatures (10-12°C) caused the same higher pressure pain threshold to be reached in a half to two thirds the time taken at the higher temperature range of 18°C-21°C.

Discussion

In this CPT study, we observed a quasi-linear increase in the pressure pain threshold concurrently with the increased number of cold-water immersions for healthy subjects. A similar result was obtained in our previous study in which the intervals between immersions were much longer (5 and 15 minutes) [10]. Although the duration of the experiments in this study were much shorter.- 22 minutes, which included 10 immersions versus 4 or 6 immersions with intervals of 5 and 15 minutes between immersions, respectively. We observed a similar rise in the pressure pain threshold that reached 9 to 9.5Pa by the end of the experiment (Figure 7). From these results we conclude that while temperature appears to be the primary driving force in regard to the magnitude of habituation, even temperatures as high as 20°C (Figure 6) will provide a large amount of habituation given sufficient time. If temperature were the sole local parameter controlling decreased pain sensitivity, and peripheral dampening of the skin pain receptors were the main mechanism for causing habituation, then the surface temperature of the arm ought to correlate with the pain threshold. In our experiments we do observe such a general correlation, but apparently the same effect at ap-

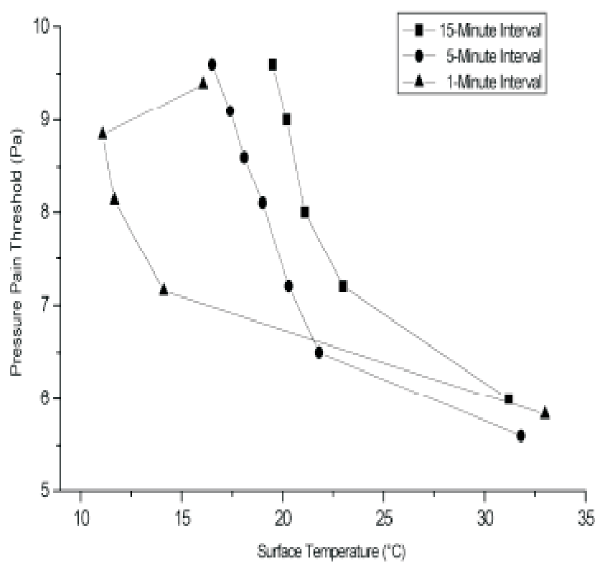

Figure 6
Correlation using mean values between surface temperature and pressure pain threshold for this study and incorporating data from the study of Kalpakcioglu et al. [10]

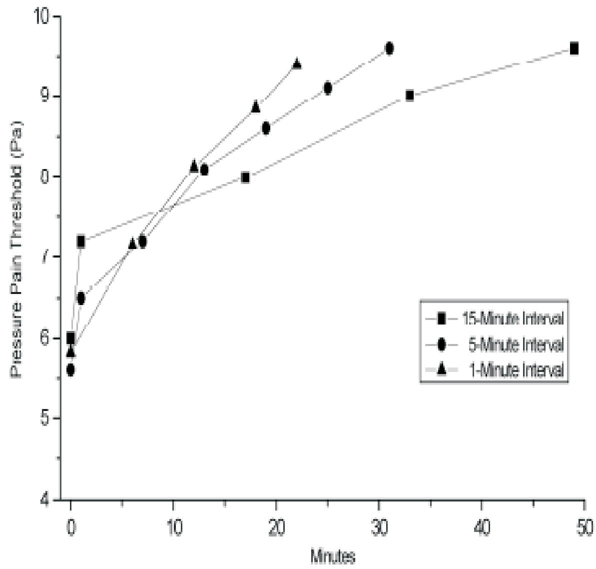

Figure 7
Correlation of time and mean values of pressure pain threshold for this study and incorporating data from the study of Kalpakcioglu et al. [10].

proximately 12-15°C can be seen at 20-23°C if sufficient time is allowed. This argues against a simple temperature-proportional dampening effect, and might suggest that neuron inhibition at the segmental level of the spinal cord by afferent non nociceptive fibers is also possible.

The phenomenon of cold habituation is primarily triggered at the level of the medulla oblongata [13] via afferent pathways from the cooled site. However, the results of other investigators suggest that control of habituation is a complex process that comprises local as well as central nervous system (CNS) components. For example, both Tamura and An [9] and Huizenga et al. [14] noted that in healthy subjects, following cooling there is a compensatory rise in core temperature, which has an affect on how the cold sensation induced by immersion is perceived. However, Jansky et al [15], who immersed the legs of healthy volunteers in cool (12°C) water, also noted that skin temperatures of the non-cooled parts of the body undergo a "mosaic of dynamic changes", which included cycles of cold-induced vasodilation, and minute cycles in the forehead, thighs and chest, that were in synchrony with the heart rate, indicating a permanent, generalized but discontinuous control of vasomotion by the sympathetic nervous system during local cooling. The authors concluded, "initial vasoconstrictor response is being controlled independently of the central temperature input." The CPT-induced sympathetic response gives rise to separate responses in the central versus the peripheral circulation, with the response in the former larger than in the latter [16]. In general, the response of arterial pressure to the CPT is higher and much more consistent than heart rate, which is partially reflected in our study. For example, Mourot et al [2] reported that only 51% of their subjects had a sustained heart rate response, while in the other subjects, heart rate decreased after an initial increase. We have observed similar results in both of our studies, although more of our subjects had sustained heart rate increases. It was also noted in the study of Mourot et al [2] that a higher sympathetic response at the skin level during the CPT was observed for this second group with the decreased heart rate.

Kregel et al- [17] suggested that the increase in MNSA (muscle sympathetic nerve activity) that occurs during the CPT is driven by high-threshold nociceptive fibers in the cooled body part, primarily achieved by the C polymodal fibers when the skin temperature falls below 15°C, which in our experiments was only achieved when the interval between cold water immersions was 1 minute. Experiments carried out by Cui et al. [3] also confirm that baroreceptors are still capable of modulating heart rate and muscle sympathetic nerve activity during the CPT, but while the sensitivity of baroreflex modulation of MSNA is enhanced, the sensitivity of heart rate modulation remains unchanged.

In their study, Yarnitsky and Ochoa [18] noted that when they blocked the myelinated A delta cold-specific fibers so that cold sensation was abolished and then further decreased the temperature, a sensation of burning pain and significant decrease in pain threshold was observed, which they explained through the removal of inhibitory primary afferent input. These results were in accordance with previous evidence that pain suppression at low temperatures was caused by central gating of cold-specific input on nociceptor input. While our results do not contest this theory, they do show that pain suppression and habituation can occur over a wide range of temperatures, and that combinations of sensory input from the skin and muscle are likely involved through different mechanisms. Our results also have a number of clinical implications with regard to the treatment of pain through cryotherapy and hydrotherapy, and provide some guide to the affects of temperature, time, and likely increase in pain threshold.

References

1. Velasco M, Gomez J, Blanco M, Rodriguez I. The cold pressor test: pharmacological and therapeutic aspects. Am. J. Ther, 1997; 4, 34-38

2, Mourot L, Bouhaddi M, Bussuges A, Regnard J. Autonomic cardiac control during the cold pressor test in normal subjects. Physiol. Res. 2008; Jan 17 [Epub ahead of print].

3. Cui J, Wilson TE, Crandall CG, Baroreflex modulation of muscle sympathetic nerve activity during cold pressor test in humans. Am. J. Physiol. Heart. Circ. Physiol. 2002; 282, H1717-H1723.

4.Kowalczyk WJ, Evans SM, Bisaga AM, Sullivan MA, Comer SD. Sex differences and hormonal influences on response to cold pressor pain in humans. J. Pain 2006; 7, 151-16

5. Washington LL, Gibson SJ, Helme RD. Age-related differences in the endogenous analgesic response to repeated cold water immersion in human volunteers. Pain 2000; 89, 89-96.

6. Stening K, Eriksson O, Wahren L, Berg G, Hammar M, Blomqvist A. Pain sensations to the cold pressor test in normally menstruating women: comparison with men and relation to menstrual phase and serum sex steroid levels. Am. J. Physiol. Regul. Integr. Comp. Physiol. 2007; 293, R1711-R1716.

7. Polianskis R, Graven-Nielsen T, Arendt-Nielsen L. Modality-specific facilitation and adaptation to painful tonic stimulation in humans. Eur. J. Pain 2002; 6, 475-484.

8. Catz A, Bluvshtein V, Korczyn AD, Pinhas I, Gelernter I, Nissel T, Vered Y, Bornstein NM, Akselrod S. Cold pressor test in tetraplegia and paraplegia suggests an independent role of the thoracic spinal cord in the hemodynamic responses to cold. Spinal Cord 2008; 46, 33-38.

9. Tamura T, An MY. Physiological and psychological thermal response to local cooling of human body. J. Therm. Biol. 1993; 18, 335-339.

10, Kalpakcioglu B, Gokpinar CE, Khani A, Gutenbrunner C, Fischer MJ. Effects of repeated immersion of the forearm in cold water on the habituation of pain thresholds in healthy subjects. Thermol Int 2008; 18: 51-56

11.Pedersen JL, Keheler H. Hyperalgesia in a human model of acute inflammatory pain: a methodological study, Pain 1998; 74: 139-151

12. Fowler CJ, Sitzoglou K, Ali Z, Halonen P. The conduction velocities of peripheral nerve fibres conveying sensations of warming and cooling. J. Neurol 1988; 51:1164-1170

13. Mizushima T, Tajima F, Nakamura T, Yamamoto M, Lee KH, Ogata H. Muscle sympathetic nerve activity during cold pressor test in patients with cerebrovascular accidents. Stroke 1998; 29, 607-612.

14.Huizenga C, Zhang H, Arens E, Wang D. Skin and core temperature responses to partial- and whole-body heating and cooling. J. Thermal Biol. 2004; 29, 549-558.

15. Jansky L, VavraV, Jansky P, Kunc P, Knizkova I, Jandova, D, Slovaek K. Skin temperature changes in humans induced by local peripheral cooling. J. Thermal Biol. 2003; 28: 429-437.

16. Casey DP, Braith RW, Pierce GL. Changes in central artery blood pressure and wave reXection during a cold pressor test in young adults. Eur J Appl Physiol 2008; 103:539–543

17. Kregel KC, Seals DR, Callister R. Sympathetic nervous system activity during skin cooling in humans: relationship to stimulus intensity and pain sensation. J. Physiol. 1992; 454, 359-371.

18, Yarnitsky D, Ochoa JL. Release of cold-induced burning pain by block of coldspecific afferent input. Brain 1990; 113, 893-902.

Address for Correspondence

Michael J. Fischer, MD

Department of Physical and Rehabilitation Medicine (OE8300), Hannover Medical School,

Carl-Neuberg-Strasse 1, D-30625 Hanover, Germany

Telephone: +49-511-532-4100; fax: +49-511-532-4293

Email: fischer.michael@mh-hannover.de

(Manuscript received 10.7.2008, accepted on 2.10.2008)

21st Thermological Symposium of the Austrian Society of Thermology Recent Advances in Thermology

15th November 2008, Goldener Saal, SAS Raddisson Hotel, Vienna, Parkring 16

Programme

Chair: Prof Dr Kurt Ammer (Austria), Prof Dr. Anna Jung (Poland)

9.00	*R.Vardasca*, U.Bajwa (Portugal/Pakistan)	Impact of Noise Removal Techniques on Measurement in Medical Thermal Images
9.15	Discussion	
9.20	B.Jesenšek Papež, *M.Palfy,* ZTurk (Slovenia)	Thermal Imaging As A Diagnostic Tool In Carpal Tunnel Syndrome
9.35	Discussion	
9.40	*R.Thomas* (UK)	Minimum Specification for Medical Thermal Imagers
9.55	Discussion	
10.00	*E.F.J,Ring* (UK)	Screening for Fever by Thermography
10.25	Discussion	
10.30	*J. B. Mercer* (Norway)	Infrared Thermography in semi-free ranging domesticated African Elephant (*Loxodonta africana*) - preliminary results from a pilot study.
11.00	Discussion	

11.05-11.35 Coffee Break

Chair: Prim Dr T.Schartelmüller (Austria), Prof Dr F.Ring (UK)

11.35	*K Amme*r (Austria)	Thermal imaging for the diagnosis of primary Raynaud´s Phenomenon
11.55	Discussion	
12.00	TA Buick, KJ *Howell* R. Gush, CP Denton , RE Smith (UK)	A Comparison of Infrared Thermography (IRT) and Full-Field Laser Perfusion Imaging (FLPI) For Assessment of Hand Cold Challenge and Dermal Inflammation
12.20	Discussion	
12.25	*G. Litscher* (Austria)	Thermal imaging and related techniques in acupuncture research
12.55	Discussion	
13.00	*R.Vardasca*, (Portugal)	Symmetry of temperature distribution in the upper and the lower extremites
13.20	Discussion	
13.25	*Adriana Nica* Ana Meila, Clara Dima (Romania)	Monitoring Treatment in Patients after Stroke by Thermal Imaging: Study Design
13.50	Discussion	
13.55	*Carolin Hildebrandt* C.Raschner(Austria)	Thermal Imaging as Screening Tool for Knee Injuries in Professional Junior Alpine-Ski-Racers In Austria
14.15	Discussion	

14.30 Close

Abstracts

THERMAL IMAGING FOR THE DIAGNOSIS OF PRIMARY RAYNAUD´S PHENOMENON

K Ammer,

Institute for Physical Medicine and Rehabilitation, Hanuschkrankenhaus, A- 1140 Vienna, Austria

Primary and secondary Raynaud´s Phenomenon differ in etiology, severity and location of symptoms Although about 20 % of patients with primary Raynauds phenomenon may undergo transition to a secondary form of this vasospastic disease, a rough differentiation between primary and secondary Raynaud´s phenomenon can be made by the number of involved fingers. Primary vasospastic disease affects by definition all fingers, but with less severe symptoms. Secondary Raynaud´s may involve some single or all fingers with occasionally severe signs of the transient reduction of perfusion. The diagnosis Raynaud´s phenomenon requires attacks of triphasic colour changes of fingers, however, patients with primary Raynaud´s present often only with blanching and coldness or biphasic colour changes of all fingers.

Between 1st November 2007 and 6th October 2008 thermograms of both hands were recorded from 85 patients suspected of Raynaud´s phenomenon. After acclimatization for 15 minutes to a room temperature of 24 degrees, the hands were positioned on a table, and images in the dorsal view for both hands were recorded. Then the hands, covered with plastic gloves, were fully immersed for 1 minute in water of 20°C. Immediately after taking off the gloves, and at in interval of 10 minutes 3 other thermal images were captured. Spot temperatures were measured on the tip and over the mid of metacarpal bone of each finger. Gradients were calculated by subtracting the metacarpal temperature from the temperature of the finger. Raynaud´s phenomenon was diagnosed when negative temperature gradients > 1° were detected 20 Minutes after the cold challenge. Involvement of all fingers with thumbs either included or excluded was regarded as primary Raynaud´s phenomenon.

68 females (age range: 14 to 81 years) and 17 males (age range: 17 zo 81 years) were investigated. In total, 47 patients (5 males, 42 females)were diagnosaed as primary Raynaud´s phenomenon, 24 subjects (3 males, 21females) showed involvement of single fingers and the remaining 24 subjects (9 male, 15 females) presented with normal temperature recovery after the cold challenge.

A higher proportion of females than males presented with thermographic signs of Raynaud´s phenomenon. Involvement of all fingers, was a common finding in our sample . Primary Raynaus´s phenomenon was not restricte to young age, as slow recovery of temprature after cold challenge was detected in all fingers in 6/13 patients aged 70 years or older.

THERMAL IMAGING AS A DIAGNOSTIC TOOL IN CARPAL TUNNEL SYNDROME

Jesenšek Papež B., Palfy M., Turk Z.

University Clinical Centre Maribor, Ljubljanska 5, Maribor, Slovenia

INTRODUCTION:Thermography is a type of infrared imaging, capable of detecting radiation in the infrared range of the electromagnetic spectrum (0.9–14μm) and producing images of that radiation. In carpal tunnel syndrome at earlier stages of syndrome vasoconstriction is common, while at later vasodilatation. Consequently, unexpected skin temperatures can be measured at different parts of affected hand.

AIM: The aim of present study was to use a software-based intelligent system for diagnosis of carpal tunnel syndrome. Artificial neural networks, known as a well established data mining technique, were used for thermal image analysis.

METHODS:28 patients and volunteers participated in creating our image database, resulting in 44 images of hands. There were 23 images of hands belonging to patients with the carpal tunnel syndrome of different severities and 21 images of healthy hands. Images were taken with the Avio's Neo Thermo TVS-700 camera with resolution of 320x240 pixels. The software application we developed for the purposes of this study consists of two modules. First module takes care of image segmentation and extraction of temperature readings while the second one performs the image analysis and tries to diagnose the carpal tunnel syndrome.

RESULTS AND DISCUSSION: Classification success rates exceed 75% in most cases. However, it should be noted that only 44 images were at our disposal, which is a very small number, taking into consideration the importance a learning process plays in artificial neural networks development. When operating with such small sets of objects the classification results can be misleadingly good (or bad). Only when our image database will grow considerably a real assessment of results will be possible.

Table : Classification success rate compared to the reference case

no.	Included segments	Success rate (%)
1	all dorsal segments (reference case)	80.6%
2	all segments	74.3%
3	all palmar segments	65.6%
4	all dorsal but 1st finger (thumb)	81.8%
5	all dorsal but 2nd finger	77.3%
6	all dorsal but 3rd finger	81.8%
7	all dorsal but 4th finger	79.2%
8	all dorsal but 5th finger	75.2%
9	all dorsal without 2nd and 5th finger	70.8%
10	all dorsal without 1st, 2nd and 3rd finger	64.5%
11	all dorsal without wrist segments	82.5%
12	all dorsal without metacarpal segments	78.4%

CONCLUSION:The development of thermal imaging technology and involvement of intelligent systems enabled new possibilities which were previously unavailable. It is our goal to research these possibilities and determine whether thermal imaging can be used as a diagnostic tool in nerve entrapment syndromes.

SCREENING FOR FEVER BY THERMOGRAPHY

E.F.J. Ring (UK)

Medical Imaging Research Unit, Faculty of Advanced Technology, University of Glamorgan, Pontypridd, UK

A new draft standard ISO/IEC TC 121/SC 3/WG 8-PT1 has been drawn up to provide a working specification for a "screening thermograph". The deployment of infrared imaging in airports and ports began with the SARS outbreak in the Far East, and is still in operation at some airports.

The writing group for this new document have considered the many facets of the technology, and its application where numbers of people have to be screened in a short time. Should a fever pandemic arise, local public health authorities will have the right to enforce restrictions on the movement and travel of anyone with a raised temperature, particularly to an area or country known to be affected by the outbreak of infection.

Two new documents have been prepared; both are based on the standards publication from Singapore (SPRING). The overall requirements are for a calibrated radiometric camera system designed specifically for rapid screening (probably height adjustable), and able to image the area of the frontal face with the highest possible resolution. The area around the eyes, with the specific target of the inner canthi . The standard describes performance tests for the manufacturer, and in a part two document, the deployment, implementation and operational guidelines are described.

The optimal imaging technique requires the subject to be positioned close to the camera system, looking directly ahead. The designers of the screening thermograph may use an audible and /or visible alarm if the subject has a raised temperature. Any subjects who fail the normal test, are likely to be subjected to a clinical screen, and clinical thermometry used to confirm the presence of fever.

As each installation will require the camera to operate continuously, uncooled detector systems are considered to me more suitable, to avoid expensive refurbishment of the cooling system. Many adjustable settings on a commercial thermal imaging system will need to be inactivated. One example is the emissivity setting, which should be fixed, and not capable of being accidentally changed by an inexperienced operator. An external reference source is also specified, as a visible check on the sable operation of the camera.

A glossary of terms is included in the document, and many aspects of the draft documents refer to existing standards for electrical safety, and those affecting medical instrumentation. The screening thermograph is described as a clinical device.

IMPACT OF NOISE REMOVAL TECHNIQUES ON MEASUREMENT IN MEDICAL THERMAL IMAGES

Vardasca, R.[1], Bajwa U.[2]

[1]Medical Imaging Research Unit, Department of Computing and Mathematical Sciences, Faculty of Advanced Technology, University of Glamorgan, Pontypridd, Rhondda Cynon Taff, CF37 1DL, Wales, United Kingdom
[2] Department of Computer Engineering, Center for Advanced Studies in Engineering, 19-Attaturk Avenue, G-5/1, Islamabad, Pakistan

Medical infrared (IR) images are sensitive to noise. It affects directly the temperature measurements of the objects in a scene. There are documented noise removal techniques that have good performance on digital images but will produce different results for each technique on temperature readings from thermal images.

Twenty noisy images were selected from a database and after being processed with several noise removal techniques, the result was statistically analysed. That analysis includes maximum temperature, minimum temperature, mean temperature and standard deviation of same region of interest and Root mean square error, Signal to noise ratio and cross correlation coefficient of each resultant image. In the end all techniques are compared and graded.

This investigation shows that all techniques produce different results, the recommended method for improving medical thermal images are the Median, Mean and Wiener filters. Results however suggest that noise filtering should only be applied when specifically needed.

INFRARED THERMOGRAPHY IN SEMI-FREE RANGING DOMESTICATED AFRICAN ELEPHANTS (*LOXODONTA AFRICANA*) - PRELIMINARY RESULTS FROM A PILOT STUDY. *

Philippa Hidden, Andrea Fuller, Linda Fick, James B. Mercer*

School of Physiology, University of the Witwatersrand, Johannesburg, South Africa. and *Department of Medical Physiology, Faculty of Medicine, UiTø, Tromsø, Norway

* Reprint from Thermology international 2008, 18(2) 59

Infrared (IR) thermal images of semi-free ranging domesticated African elephants were taken at selected intervals over a 24 hour period during summer (March). The animals belonged to a small herd consisting of 5 adults and a 6-month old juvenile housed at the Letsatsing Game Reserve, North West Province, South Africa. The reserve includes a visitor's centre situated beside a wallow plus stabling and maintenance facilities. The adults are used for elephant back riding safaris that run only in the morning and late afternoons. The herd spends much of the rest of the day-light hours browsing naturally, pursuing a lifestyle similar to wild elephants. At night time the animals are kept in individual concrete stalls in an open sided high roofed stabling area. In addition to recording IR-thermal images, body core temperature in 2 individuals was continuously measured using ingested temperature data loggers. The data loggers were recovered from the faeces following a passage time through the intestinal tract of ca. 42 and 72 hours respectively. Meteorological data, including air temperature, black globe temperature and solar radiation were continuously measured from a local field station. Written details of the animals behavioural patterns were also recorded throughout the daylight hours. The IR-images were taken using a FLIR ThermaCam S65 and FLIR SC3000 cameras (FLIR Systems AB, Boston,MA, USA). All images were electronically stored and afterwards processed using image analysis software ThermaCAM Researcher Pro 2.8 SR-1 (FLIR Systems AB). IR thermal images of the elephants were taken at different times of the day and included activities at the wallow, while grazing in the bush, before and after the rides, and in the stables shortly before sunrise and shortly after sun-down. Preliminary results will be presented in which the thermal state of the animals as shown in the IR-thermal images will be related to both body core temperature and the meteorological data throughout the 24 hour period.

THERMAL IMAGING AND RELATED TECHNIQUES IN ACUPUNCTURE RESEARCH

G. Litscher

Research Unit of Biomedical Engineering in Anesthesia and Intensive Care Medicine and TCM Research Center Graz (http://tcm-graz.at), Medical University of Graz, Austria

Quantitative thermal imaging is becoming an important method in acupuncture research. Using infrared thermography we evaluated the effects of changes in peripheral temperature during the initial phase of manual needle and laser acupuncture under standardized conditions. According to Traditional Chinese Medicine (TCM), the combination of the acupoints Neiguan (Pe.6) and Quchi (LI.11) leads to a general increase in energy and is applied when circulatory problems in the upper extremities are present (1,2). In this presentation, examples of thermography and related techniques, e.g. laser Doppler imaging (LDI) for measuring changes of microcirculation, will be demonstrated. In addition, a new method for moxibustion will be introduced. Thermography and LDI were used to standardize this innovative method.

There are many possible uses of thermal imaging in the field of TCM in general and acupuncture research in particular, but there are still methodological limitations of this modern measuring procedure. The validity of the method for proving meridian structures according to the view of TCM must be considered critically and analyzed scientifically (3,4).

Thermographic methods such as infrared cameras and other high-tech methods like LDI are effective tools for the visualization of effects in acupuncture research which support demystification of this ancient medical treatment method.

Acknowledgements: The studies were supported by the Zukunftsfonds Steiermark (4071), the BMWF, the BMGFJ (Sino-Austrian research project) and 3B Scientific, Hamburg.

References

1.Litscher G. Bioengineering assessment of acupuncture, part 1: thermography. Crit Rev Biomed Eng 2006;34(1):1-22.

2.Litscher G, Wang L. Thermographic visualization of changes in peripheral perfusion during acupuncture. Biomed Tech 1999;44(5) :129-34.

3.Litscher G. Infrared thermography fails to visualize stimulation-induced meridian-like structures. Biomed Eng Online 2005;4:38. URL: : http://www.biomedical-engineering-online.com/content/4/1/38

4.Litscher G, Ammer K. Visualization of equipment dependent measurement errors, but not of meridian-like channels in complementary medicine – a thermographic human cadaver study. Thermology International 2007;17(1):32-35.

A COMPARISON OF INFRARED THERMOGRAPHY (IRT) AND FULL-FIELD LASER PERFUSION IMAGING (FLPI) FOR ASSESSMENT OF HAND COLD CHALLENGE AND DERMAL INFLAMMATION

Buick TA[1], Howell KJ[2], Gush R[3], Denton CP[2], Smith RE[1]

Departments of [1]Medical Physics and [2]Rheumatology, Royal Free Hospital, London. NW3 2QG. UK.
[3]Moor Instruments, Axminster, Devon. EX13 5HU. UK

IRT is a well-established technique for the assessment of the response of the hand to cold challenge (1) and of dermal inflammation (2), as it offers full-field dynamic imaging of skin. However, the radiometric measurement of skin temperature is only a surrogate for the dermal microcirculation – a parameter of interest: many factors besides blood flow can influence skin temperature, and these limit the utility of IRT as a microvascular tool (3).

Full-field laser perfusion imaging (FLPI) is a newly-available commercial technique offering many of the advantages of IRT (full-field image, fast dynamic response), but, in contrast, the signal is derived directly from red cell blood flux in the skin (4). The utility of FLPI for the assessment of cold-induced peripheral vasospasm or dermal inflammation is, as yet, to be evaluated.

The two techniques were used simultaneously for the assessment of hand cold challenge (water at 15°C for one minute) in 3 healthy subjects. We also used the two devices to record the inflammatory skin response at the forearm of a healthy subject after a light scratch. We will present a narrative comparison of IRT and FLPI.

FLPI shows promise as a microvascular imaging tool, and indeed may have benefits over IRT for the assessment of skin inflammation. Larger studies of the utility of FLPI in healthy and diseased subjects are now required. Potential applications, benefits, and limitations will be discussed.

References

1.Foerster J, Kuerth A, Niederstrasser E, Krautwald E, Pauli R et al. A cold-response index for the assessment of Raynaud's phenomenon. J Dermatol Sci 2007 Feb;45(2):113-120

2.Martini G, Murray KJ, Howell KJ, Harper J, Atherton D et al. Juvenile-onset localized scleroderma activity detection by infrared thermography. Rheumatology (Oxford) 2002 Oct;41(10):1178-1182

3.Howell KJ, Dziadzio M, Smith RE. Thermography in Rheumatology. In Thomas RA (ed). Proc 6 Int Conf QRM, 2007, Coxmoor Publishing, pp174-178

4.Briers JD. Laser Doppler, speckle and related techniques for blood perfusion mapping and imaging. Physiol Meas 2001 Nov;22(4):R35-66

SYMMETRY OF TEMPERATURE DISTRIBUTION IN THE UPPER AND THE LOWER EXTREMITIES

Ricardo Vardasca

Medical Imaging Research Unit, Faculty of Advanced Technology University of Glamorgan, Pontypridd, RCT, CF37 1DL, United Kingdom

Infrared thermal imaging is being increasingly utilised in the study of neurological and musculoskeletal disorders. In these conditions data on the symmetry (or the lack of it) of skin temperature provides valuable information to the clinician. The last major study on thermal symmetry, however, was made in 1988 and no studies have been carried out with the current generation of higher resolution cameras, especially none that compares total body views with close-up regional views in both anterior and dorsal visualisations.

In this study skin temperature measurements have been carried out using thermograms of 35 healthy subjects. Measurements were obtained from an infrared camera using the CTHERM application developed at the authors' research unit. CTHERM is capable of calculating statistical data such as temperature averages and standard deviation values in corresponding areas of interest on both sides of the body. Results show that in healthy subjects the overall temperature symmetry difference was at most 0.25°C ± 0.2ºC in total body views and 0.2ºC ± 0.15ºC in regional views. Total body views and regional views produced comparable results although better results were achieved in regional views. Using a high-resolution camera the study achieved better results on thermal symmetry in normal subjects than previously reported. Symmetry assumptions can therefore now be used with higher confidence when assessing abnormalities in specific pathologic states.

MONITORING TREATMENT IN PATIENTS AFTER STROKE BY THERMAL IMAGING: STUDY DESIGN

Adriana Nica, Ana Meila, Clara Dima

National Institute of Rehabilitation, Physical Medicine & Balneoclimatology, University of Medicine "Carol Davila. Bucharest, Romania

INTRODUCTION: Romanian medical thermography started 30 years ago in oncology, but in the late 3 years extended to other medical domains as functional investigation of thyroid, diabetes etc.

The patient with stroke has central motor deficiency and peripheral vascular anomalies. Vegetative vascular reactivity is followed by an adaptation response, peripheral thermoregulation, under the command of neuro-vegetative, metabolic, systemic and local factors.

SAMPLE: Our study has had in view a group of 10 patients with stroke, hospitalized in the University Clinic of National Institute of Rehabilitation, Physical Medicine and Balneology Bucharest, Romania. We used thermography to observe the thermic differences between the right and left limbs of the patients and the thermic dynamic before and after the treatment.

METHOD: The patients were clinico-functional evaluated and respecting the inclusion criteria: time after the acute cerebro. vascular event, localisation of symptoms, ability to stand or walk, treatment modalities (respecting a homogene pharmacologic and non-pharmacologic treatment). The patients were evaluated analyzing the predominant pathology of the upper and lower limb, right or left dominant limb and the parameters Barthel-Index, FIM, Motility Index, strength of the maximum affected muscles of the upper and the lower extremity.

We captured the thermal images of the body according to the Glamorgan Protocol before and after the treatment and we statistical process the dates.

Even if the study was on a small number of patients it showed the thermic differences by the motor hemi body deficiency and two patients had more important thermic (and X-rays) differences showing reflex reaction in algic complex syndrome type II.

For Romanian Medical Rehabilitation this clinical study opens a new perspective for functional stroke investigation.

THERMAL IMAGING AS A SCREENING TOOL FOR KNEE INJURIES IN PROFESSIONAL JUNIOR ALPINE-SKI-RACERS IN AUSTRIA

C. Hildebrandt, C. Raschner

Department of Sport Science, University of Innsbruck, Austria

INTRODUCTION:Knee injuries, especially ACL ruptures, represents a major problem in professional alpine skiing. According to TECKLENBURG K.(2005) et al 53,8% of all female skiers in the Austrian Junior National Team have sustained an ACL rupture. The incidence of ACL ruptures in male skiers is slightly lower.

Although it is important to improve rehabilitation methods for the treatment of knee injuries, preventing is even better.

In recent years, *Thermal Imaging* has been successfully utilized in the field of veterinary medicine by detecting locomotion injuries in race horses and to monitor the health status (HARPER D.L. 2000).

However, despite similar anatomy and physiological pattern, only few investigations have been conducted for the prevention and detection of knee injuries in athletes with *Thermal Imaging*.

AIM: The general aim of the study is therefore to investigate the use of *Thermal Imaging* as an appropriate assessment in terms of knee injury prevention and diagnostic in young alpine ski racers. Knowing that the temperature distribution of the knee in healthy subjects is highly symmetrical from the right to the left side, our specific purpose is to evaluate interindividual local temperature variations in conjunction with reported symptoms, knee pain and previous injuries.

It is assumed that ski racers knees are exposed to much physical stress during their competition season. Therefore the analysis of a pre- and postseason measurement is required and may enhance the detection and localisation of thermal changes before they become clinically.

METHODS: In the first stage a pilot study with 53 students was carried out to establish an appropriate protocol, to define a reference of normal thermogramms including the typical range and distribution of knee temperature and last but not least to define the region of interest and most suitable standard view. An infrared camera (TVS 500EX) and the appropriate software (iReport) was provided from the Germany company GORATEC GmbH.

After an acclimatisation period of 20minutes an image of the anterior/posterior and medial/lateral aspect of both knees were recorded. The thermal environment remained under constant conditions.

The findings and the definition of the best conditions from the first part of the study will be used in the second stage, in which 50 young ski racers (male and female, 14-19 years) from the "Skigymnasium Stams" will be tested. A questionnaire, the examination by a physiotherapist and the medical history, obtained from a sports medicine specialist, will complete the findings of the images.

RESULTS/DISCUSSION:By means of some case studies from the first testing period of non injured and previously injured subjects, local temperature variations and thermal anomalies in conjunction with the medical history and the best standard view of the knee will be discussed.

Furthermore, based on a few examples from patients suffering on an acute ACL rupture or knee injury, thermal imaging as an outcome measure of monitoring the magnitude of injury will be discussed.

Meetings

15th November 2008

21st Symposium of the Austrian Society of Thermology, SAS Hotel Vienna, Austria

Topic: Recent Advances in Thermology

Confirmed speakers Prof F. Ring, UK
Prof. A.Nica, Romania
Dr. R.Thomas. UK
K. Howell, UK
Prof.K.Ammer, Austria
Prof. G.Litscher, Austria
C. Hildebrandt, Austria
Dr. B. Jesenek-Papez, Slovenia
R.Vardasca, Portugal
Prof. J.Mercer, Norway

Information
Prof K. Ammer, MD, PhD
Austrian Society of Thermology
Hernalser Hauptstr 209/14
Email: KAmmer 1950@aol.com

29. November 2008

DGTR / IMVT Adventseminar 2008 in Mörfelden

Bürgerhaus Mörfelden, Westendstraße 60,
64546 Mörfelden-Walldorf bei Frankfurt

Workshop fee: 90,- Euro
Including storage media with presentations; coffee and lunch, certification of attendance

09:00 Opening, Topics and Issues - Becker, Berz, Sauer

Session 1: Basics of IR imaging

09:10 Basics of measurement for medical IR imaging Orglmeister

09:30 Human thermal profiles and patterns and clinical correlations - Sauer

Session 2: – Breast IR imaging

09:50 from early breast thermography to recent infrared imaging - Berz

10:10 Typical patterns of breast cancer (case reports) Sauer

10:40 *Coffee Break, Exhibition*

11:00 Comparing established breast examinations with IR imaging - Schulte-Uebbing

11:20 How false are false-positive results (Breast IR imaging)? - Berz

11:40 Preventive aspects of breast IR imaging - breast health issues - Sauer

12:00 Standardisation, fine tuning and increase of reliability (breast IR imaging) - Berz

12:20 Discussion, future development of BreastIR imaging Schulte-Uebbing

13:00 *Lunch Break, Exhibition*

Session 3: Locomotor IR imaging

14:00 Thermal patterns and functional locomotor diagnosis Ammer

14:20 Experiences with IR imaging in an orthopaedic hospital - Steinlein

14:40 Visualization of chirotherapeutic treatment using IR imaging - Helling

15:00 Research project: IR imaging of M. Raynaud Goetze

15:20 *Coffee Break, Exhibition*

Session 4: Contact thermography and infrared spot measurement

15:50 Rost's contact Thermography and Sauer's infrared spot measurement - Sauer

Session 5: Infrared Imaging – Education, Training and Certification

16:10 The DGTR/IMVT-Program for Mediical Education Infrared Imaging - Berz

16:30 Final discussion

17:00 *Close*

Speakers

Prof. Dr. med. Kurt Ammer PhD,
Hanuschkrankenhaus Wien,
Präsident der Österr. Gesellschaft für Thermologie,
Generalsekretär der EAT – European Association of Thermology

Peter Becker
Bürgermeister der Stadt Mörfelden-Walldorf

Prof. Dr. med. Reinhold Berz
Präsident der DGTR / IMVT, Danzig

Dr. med. Steven Goetze
Oberarzt, Abt. Experimentelle Dermatologie,
Universitätsklinik Jena

Dr med Klaus Helling
Chefarzt der Klinik für Manuelle Therapie (KMT) Hamm

Dipl.Ing. Albert Orglmeister
Geschäftsführer O-Tec Infrarotsysteme

Dr. med. Helmut Sauer
Vizepräsident der DGTR / IMVT,
Waldbronn bei Karlsruhe

Prof. Dr. med. Claus Schulte-Uebbing
Gynäkologe, München

Dr. med. Sven Steinlein
Orthopädische Klinik, Rhein-Sieg-Klink Nürnbrecht

2009

27th - 29th March 2009

13th National Congress of the Polish Association of Thermology, Zakopane, Poland

REGISTRATION FEE: 200-Euro

ABSTRACT DEADLINE January 15th 2009.

Please submit to

Prof Dr. Anna Jung
Pediatric and Nephrology Clinic,
Szaserów Str 128 00 909 Warsaw 60, POLAND
Fax (48 – 22) 6816763
Email: ajung@wim.mil.pl or a.jung@spencer.com.pl

13 — 17 April 2009

SPIE DSS Conference DS101 — Orlando World Center Marriott Resort & Convention Center, Orlando, FL United States

Information: http://www.thermosense.org/dev/

1st-3rd July, 2009

16th International Conference on Thermal Engineering and Thermogrammetry (THERMO), Budapest, Hungary

Information
Application Forms and abstracts/papers should be sent to:
Dr. Imre BENKÖ,
MATE Secretariat, House of Technology, III. 318.
H-1372 Budapest, POB. 451., Hungary
Fax: +361-353-1406, Phone: +361-332-9571.,
E-mail: mate@mtesz.hu

/eng/Pages/2009/Thermo2009/index.php and for previous 15th THERMO
/eng/Pages/2007/Thermo2007/index.php

17th -20th September 2009

Combined Conferences

11th European Congress of Medical Thermology

55th Annual Congress of the German Society of Thermography and Regulation Medicine

22nd Thermological Symposium of the Austrian Society of Thermology

Conference of the German Society of Thermology (DGT)

Venue: Region of Frankfurt/Main, Germany

Main theme: Temperature Measurement in Humans and Animals

Further information:

Prof Dr med Reinhold Berz
President of the German Society of Thermography and Regulation Medicine (DGTR)
International Medical and Veterinary Thermographers IMVT
Harbach 5
D-36115 Hilders / Rhön

Tel +49 (0) 66 81 - 72 70, Fax +49 (0) 66 81 - 85 51
Email: reinhold.berz@inframedic.de

or

Prof Dr med Kurt Ammer PhD
Austrian Society of Thermology
Hernalser Hauptstr 209/14
A-1170 Wien, Österreich

Tel & Fax: +43 1 480 54 23
Email: KAmmer1950@aol.com

Combined Conferences
11th European Congress of Medical Thermology

55th Annual Congress of the German Society ofThermography and Regulation Medicine

22nd Thermological Symposium of the Austrian Society of Thermology

17th-20th September 2009

Last Name..First Name.. Title ....

Institution ....
Street ....

ZIP Code ....City...Country ....

Phone.. Fax .... E – mail..

Title Autors Abstract

Return this form not later than May 15th, 2009 to:

Prof. Reinhold Berz
Harbach 5; D-36115 Hilders / Rhön
Email: reinhold.berz@inframedic.de

Submission by email to the following adresses is also possible:

Prof F. Ring: efring@glam.ac.uk
Prof K. Ammer: KAmmer1950@aol.com

Thermology international

Please begin my subscription to THERMOLOGY INTERNATIONAL

Return to TOC

Dr. Kurt Ammer
Österreichische Gesellschaft für Thermologie

Hernalser Hauptstr.209/14
A-1170 Wien
Österreich

Name

Address

City State Zip

Signature Date

I am a registered member of the
- ☐ Hungarian Society of Thermology
- ☐ UK Thermography Association
- ☐ Italian Association of Thermology
- ☐ Polish Society of Thermology
- ☐ German Society of Thermography
- ☐ Romanian Society of Thermography
- ☐ Brazilian Society of Thermology

This journal is a combined publication of the Austrian Society of Thermology and the European Association of Thermology (EAT) It serves as the official publication organ of the the American Academy of Thermology, the Brazilian Society of Thermology the German Society of Thermology, the UK Thermography Association (Thermology Group) and the Austrian Society of Thermology. An advisory board is drawn from a panel of international experts in the field. The publications are peer-reviewed.

For members of the societies mentioned above the subscription rate for 4 issues/year is 32.-.€ mailing costs included. All other subscribers have to pay 38.- € + 18 € for mailing outside Austria, in total 56 € (US $ 68.-)

Payment should be sent (without any charges for the European Association of Thermology) to the following bank account:Bank Austria-Creditanstal, Vienna, Austria, IBAN=AT62 1200 0009 6502 3054 / BIC=BKAUATWW

ISSN -1560-604X
Thermology international

Thermology international

Ich bestelle ein Abonnement der THERMOLOGY INTERNATIONAL

Dr. Kurt Ammer
Österreichische Gesellschaft für Thermologie

Hernalser Hauptstr.209/14
A-1170 Wien
Österreich

Name

Adresse

Ort Staat PLZ

Unterschrift Datum

Ich bin Mitglied der
- ☐ Ungarischen Gesellschaft für Thermologie
- ☐ UK Thermography Association
- ☐ Italian Association of Thermology
- ☐ Polish Society of Thermology
- ☐ Deutschen Gesellschaft für Thermographie
- ☐ Rumänischen Gesellschaft für Thermographie
- ☐ Brasilianischen Geselschaft für Thermographie

Diese Zeitschrift ist eine gemeinsame Publikation der Österreichischen Gesellschaft für Thermologie und der Europäischen Assoziation für Thermologie (EAT)

Sie dient als offizielles Publikationsorgan der Amerikanischen Akademie für Thermologie, der Brasilianischen Gesellschaft für Thermologie der Deutschen Gesellschaft für Thermologie, der Britischen Thermographie Assoziation (Thermologie Gruppe) und der Österreichischen Gesellschaft für Thermologie.

Hochangesehene Thermologen sind Mitglieder des wissenschaftlichen Beirates dieses vidierten Fachblattes.

Für Mitglieder der oben erwähnten Gesellschaften beträgt der Abonnementpreis für 4 Ausgaben inklusive Versandkosten 32.-€ . Für alle anderen beträgt der Preis 38.- € + 18 € Versandkosten außerhalb Österreichs, somit einen Gesamtpreis von 56.- €.

Die Bezahlung wird spesenfrei für den Empfänger auf das folgende Bankkonto der Europäischen Assoziation für Thermologie erbeten:
Bank Austria-Creditanstalt, Wien, Österreich,
Bankleitzahl: 12000, Kontonummer: 965023054
IBAN=AT62 1200 0009 6502 3054 / BIC=BKAUATWW

ISSN -1560-604X
Thermology international